Clemson University
College of Engineering and Science
Control and Robotics (CRB) Technical Report

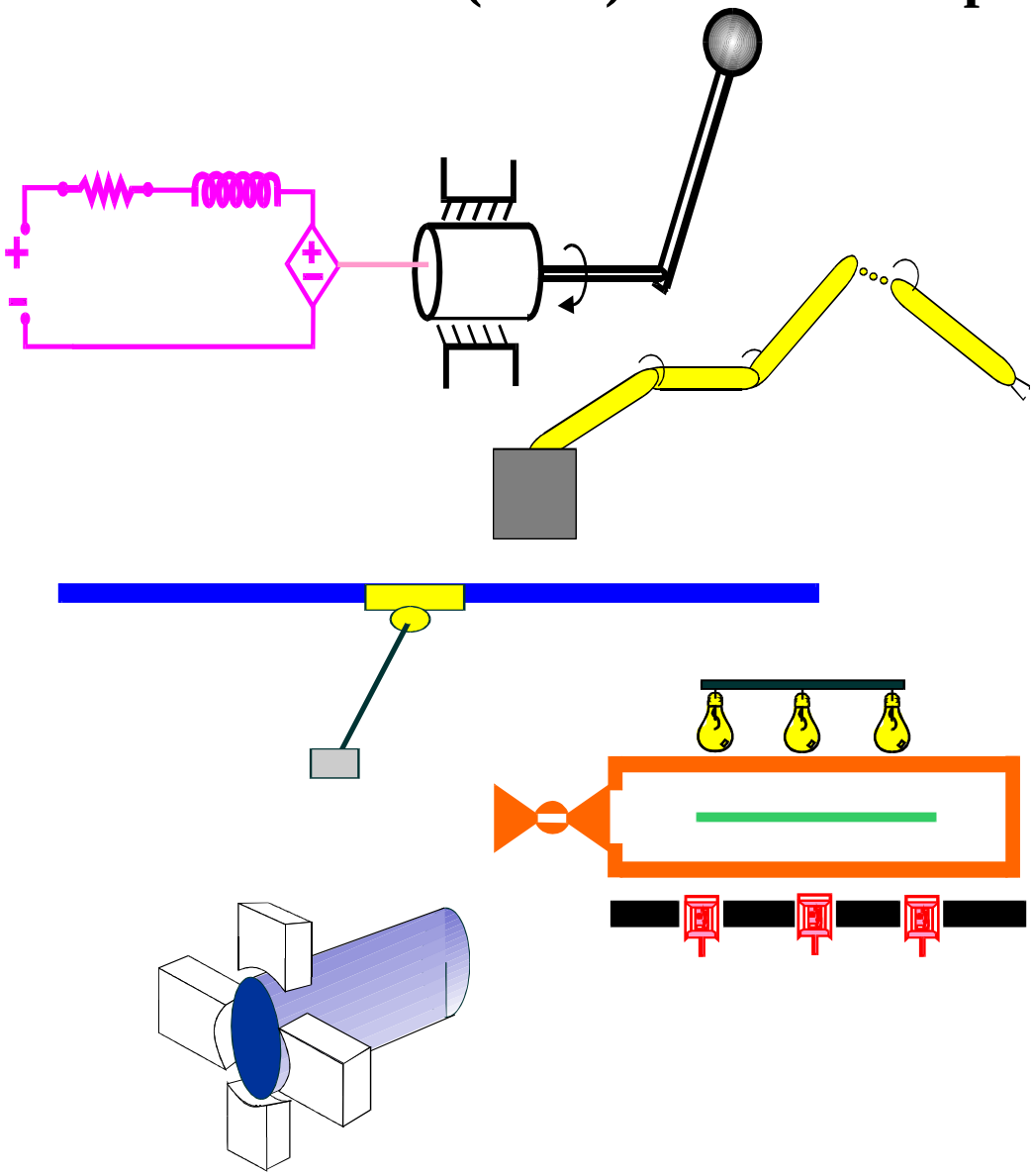

Number: CU/CRB/2/28/06/#2

Title: Output Feedback Tracking Control of an Underactuated Quad-Rotor UAV

Authors: DongBin Lee, Timothy Burg, Bin Xian, and Darren Dawson

Report Documentation Page

Form Approved
OMB No. 0704-0188

Public reporting burden for the collection of information is estimated to average 1 hour per response, including the time for reviewing instructions, searching existing data sources, gathering and maintaining the data needed, and completing and reviewing the collection of information. Send comments regarding this burden estimate or any other aspect of this collection of information, including suggestions for reducing this burden, to Washington Headquarters Services, Directorate for Information Operations and Reports, 1215 Jefferson Davis Highway, Suite 1204, Arlington VA 22202-4302. Respondents should be aware that notwithstanding any other provision of law, no person shall be subject to a penalty for failing to comply with a collection of information if it does not display a currently valid OMB control number.

1. REPORT DATE	2. REPORT TYPE	3. DATES COVERED
25 SEP 2006		**00-00-2006 to 00-00-2006**

4. TITLE AND SUBTITLE	5a. CONTRACT NUMBER
Output Feedback Tracking Control of an Underactuated Quad-Rotor UAV	5b. GRANT NUMBER
	5c. PROGRAM ELEMENT NUMBER
6. AUTHOR(S)	5d. PROJECT NUMBER
	5e. TASK NUMBER
	5f. WORK UNIT NUMBER
7. PERFORMING ORGANIZATION NAME(S) AND ADDRESS(ES) **Clemson University,Department of Electrical & Computer Engineering,Clemson,SC,29634-0915**	8. PERFORMING ORGANIZATION REPORT NUMBER
9. SPONSORING/MONITORING AGENCY NAME(S) AND ADDRESS(ES)	10. SPONSOR/MONITOR'S ACRONYM(S)
	11. SPONSOR/MONITOR'S REPORT NUMBER(S)

12. DISTRIBUTION/AVAILABILITY STATEMENT
Approved for public release; distribution unlimited

13. SUPPLEMENTARY NOTES
The original document contains color images.

14. ABSTRACT

15. SUBJECT TERMS

16. SECURITY CLASSIFICATION OF:			17. LIMITATION OF ABSTRACT	18. NUMBER OF PAGES	19a. NAME OF RESPONSIBLE PERSON
a. REPORT	b. ABSTRACT	c. THIS PAGE			
unclassified	**unclassified**	**unclassified**		**41**	

Output Feedback Tracking Control of an Underactuated Quad-Rotor UAV*

DongBin Lee[1], Timothy Burg[1], Bin Xian[2], and Darren Dawson[1]

September 25, 2006 (Updated)

Abstract

This paper proposes a new controller for an underactuated quad-rotor family of small-scale unmanned aerial vehicles (UAVs) using output feedback (OFB). Specifically, an observer is designed to estimate the velocities and an output feedback controller is designed for a nonlinear UAV system in which only position and angles are measurable. The design is performed via a Lyapunov type analysis. A semi-global uniformly ultimate bounded (SGUUB) tracking result is achieved. Simulation results are shown to demonstrate the proposed approach.

Keywords: Output Feedback, Observer, Lyapunov, Nonlinear, Quad-rotor, UAV, Underactuated

1 Introduction

The potential for unmanned aerial vehicles (UAVs) in applications as diverse as fire fighting, emergency response, military and civilian surveillance, crop monitoring, and geographical registration has been well established. Many research groups have provided convincing demonstrations of the utility of UAVs in these applications. However, there is still a large chasm between the anticipated "tool of the future" and currently available systems. The commercial and military use of UAVs is predicated on the ability of such vehicles to perform new, safer, or more cost effective tasks than traditional manned aircraft. Until recently, this has been more of a question than a statement; however, recent advances in aerial vehicle construction, sensors, digital electronics, control design have seen a rapid increase in UAV applications.

Aerial vehicle construction should be considered as an important factor in UAV acceptance and use. Materials such as carbon fiber can be used to reduce weight and improve robustness, both critical parameters in any aerial application. Improved manufacturing techniques are capable of producing small, complex, precise parts at a reasonable price and new battery technologies have made electric hovering craft more feasible. One of the interesting small aerial vehicles that seems to have benefited from these developments is the quad-rotor UAV depicted in Figure 1. The quad-rotor consists of four independently driven rotating blades that can provide lift in the vertical direction. The vehicle moves in other directions by creating a mismatch between rotor speeds, and hence, this configuration can produce torques about the roll, pitch, and yaw axes. The basic concept for the quad-rotor dates back to 1907; some notes on the history of the quad-rotor and related references

*[1]Department of Electrical and Computer Engineering, Clemson University, Clemson, SC 29634-0915, email: tburg@clemson.edu, [2]Controlled Semiconductor, FL 32819.

can be found in [1]. With this as a backdrop, the focus of the work presented here will be the small quad-rotor family of aerial vehicles. The discussion will be limited to vehicles with less than 0.5kg payload. This weight restriction means that certain technologies that may make sense for larger, more expensive aircraft may not apply to this class of aircraft.

Position, velocity, and acceleration sensing issues will begin the discussion and will serve as partial motivation for the choice of output feedback control design. From the schematic representation of a quad-rotor UAV shown in Figure 1, it can be seen that the arbitrarily positioned aircraft is fully located and oriented using three translational positions (x, y, and z) and three angles (roll - ϕ, pitch - θ, and yaw - ψ). Measurement of these six positions, the six first derivatives (velocity and angular velocity), and the six second derivatives (acceleration and angular acceleration) has proven challenging. Measuring angular and translational quantities each present different challenges. The angular velocity is perhaps the most accessible angular measurement. Angular velocity can be sensed using a mechanical gyroscope. This approach has historically yielded good results and can be scaled down in a cost effective manner. The major drawback is the moving mechanical parts may add additional weight and reduce reliability. Piezoelectric gyros have provided an alternative that does not have moving parts. More reliable gyroscopes such as the laser ring oscillator are not available for this application. Angular position may be more difficult to measure directly; however, devices such as magnetic compass, magnetometers, tilt sensors, optical horizon sensors may provide estimates of position for the roll or tilts axes, but typically have low bandwidth and poor accuracy. There are several technology options for building accelerometers to measure the angular acceleration including MEMs and piezoelectric devices.

Translational position can be directly measured with global positioning system (GPS) based systems. Enhancements, such as DGPS, are required to achieve improved accuracy. Direct sensing of the linear velocities is more difficult; an anemometer can be used to make indirect measurements that are not necessarily relative to a fixed inertial frame. An emerging alternative to the above sensors is to use vision systems to measure positions or velocities. These camera systems may be ground-based to monitor a UAV in a fixed area or may be vehicle based and used to estimate changes in scenery. Finally, it is often difficult to convert between data types with standard mathematical operations. For example, a backwards difference estimate of velocity from position information may lead to a noisy velocity signal, and integration of the velocity signal to obtain position information can rapidly accumulate error. If a trend were to be predicted based on review of literature, it would be that angular and linear positions will be more easily attained as technology evolves. This view is demonstrated in [2] where only a single GPS sensor is used to measure vehicle position and velocity for a small plane. If this trend is true, then a controller that uses only position information is well motivated.

The generally accepted end-goal that a vehicle would autonomously take-off, fly to a mission site, perform a mission, return, and land creates a daunting challenge. One of the most fundamental components of this challenge is to ensure that the craft can move to or hold a desired position and orientation. Specifically, as shown in Figure 1, the aircraft must be able to move from a current location to a new desired position (denoted by the triple x_d, y_d, z_d) and achieve a new orientation (denoted by the angles ϕ_d, θ_d, ψ_d). This low-level control objective, as it often called, is embedded at the center of high-level control objectives such as path planning, target tracking, or coordination with other crafts. Design of the low-level control represents the point at which the peculiarities of the multi-bladed UAV system must be addressed; specifically, nonlinearities of the system dynamics and the fundamental fact that the system is under-actuated. An under-actuated system is especially challenging to control since it has less control inputs than degrees of freedom, i.e. it has degrees of freedom that cannot be directly actuated. In order to achieve high overall performance, one must

address the low-level control problem. The quad-rotor UAV has six-degrees of freedom; the three translational directions and the three rotational angles; however, there are only four control inputs; the z-axis thrust and the three rotational torques. The quad-rotor UAV problem is sufficiently challenging such that many researchers have proposed control solutions based on a variety techniques that accentuate and address different aspects of the control problem. Solving the underactuated quad-rotor problem provides a choice of which degrees-of-freedom will be controlled. For example in [1], the authors use feedback linearization to explicitly control of the roll, pitch, and yaw angles and the height. Translational positions are then implicitly controlled by specification of the trajectories for the controlled axes. More typically, the translational control problem is directly addressed along with yaw angle control. For example in [4], the authors use a nested saturation algorithm. In [3], a backstepping approach to control the quad-rotor based on a model of the specific dynamics of the X4 flyer is used; this model is more complicated than that used in the other model-based designs as it includes additional terms such as gyroscopic effects of the rotating blades. In [5], the authors use a quaternion-based feedback control scheme for exponential attitude stabilization of a quad-rotor aircraft. The work given in [6], [7], and [8] are representative of vision based applications.

In this paper, a tracking controller is designed for the nonlinear dynamic model of the quad-rotor helicopter which uses only output feedback; that is, the controller operates using only position and attitude measurements. To appreciate the control design problem it is useful to consider the quad-rotor as a set of two coupled dynamic subsystems. The first subsystem contains the translational dynamics of the craft and has a single input along the z-axis direction and the second subsystem contains the rotational dynamics of the craft and contains a torque input to each of the three rotational directions; thus, the translational subsystem is inherently underactuated. The systems are coupled via the fact that the rotational velocities appear in the Coriolis force that acts on the translational subsystem – this coupling is critical as it provides the basis for the backstepping approach. The choice of control objectives can simplify or complicate the control design approach, for example, [Park] sought to control z-axis position and the three angles and thus the control inputs are already acting at the point of interest and a PID control was directly applied (neglecting nonlinearities). The choice here to control the three linear translations and the yaw angle requires that some of the torque inputs be "redirected" in order to achieve the translational tracking objectives. This work builds on previous backstepping approaches for injecting additional control action into the translational dynamics of the quad-rotor but is greatly complicated by the co-design of a velocity observer. Velocity estimation is a well known problem in the robotics literature. In [9], de Queiroz et al. make a systematic presentation of the observed integrator backstepping technique to design an observer for joint velocities in an n-link robot. In [9], it is shown that the observer and controller must actually be designed concurrently via Lyapunov stability arguments in order to ensure a stability result – a semi-global, exponential convergence of velocity estimation error and position tracking is shown for the rigid link robot. The reader is referred to this work to understand the observer and controller design and as a source of background for this technique. An additional reference for the observer design is provided to [10] where this same observer design is used but a subtlety of ensuring that all signals in the implementable form of the observer are bounded. The payoff from this approach is the mathematical assertion of semi-global, uniformly ultimately bounded tracking while compensating for system nonlinearities, estimation error, and the perturbations that result from the backstepping technique.

The paper is organized as follows. In Section 2, a well known model of the quad-rotor vehicle is presented. The assumptions and properties of this model are included. In Section 3, a velocity observer for output feedback tracking control is designed to estimate the velocities and the OFB controller using this velocity estimate is derived. Stability analyses on observer, controller, and

composite system are considered mathematically in Section 4 followed by Theorem 1 and Remark 1 which show the analysis result and the boundededness of all signals. Simulation results demonstrating the performance are presented in Section 5. Detailed developments and stability proofs are deferred to Appendices followed by a conclusion.

2 System Modeling

2.1 Quad-Rotor Aerial Vehicle Model

The quad-rotor unmanned aerial vehicle is shown in Figure 1 where it can be seen that the body-fixed reference frame, B, moves relative to a fixed inertial frame, I. The translational and rotational dynamic equations of motion in the body-fixed reference frame are [6]

$$\begin{bmatrix} mI_3 & O_{3x3} \\ O_{3x3} & J \end{bmatrix} \begin{bmatrix} \dot{v} \\ \dot{\omega} \end{bmatrix} = \begin{bmatrix} -mS(\omega) & O_{3x3} \\ O_{3x3} & S(J\omega) \end{bmatrix} \begin{bmatrix} v \\ \omega \end{bmatrix} + \begin{bmatrix} N_1(v) \\ N_2(\omega) \end{bmatrix} + \begin{bmatrix} G(R) \\ O_{3x1} \end{bmatrix} + \begin{bmatrix} B_1 & O_{3x3} \\ O_{3x1} & B_2 \end{bmatrix} \begin{bmatrix} u_1 \\ u_2 \end{bmatrix} \tag{1}$$

where $v(t) \in \Re^3$ denotes the linear velocity, $\omega(t) = [\omega_x, \omega_y, \omega_z]^T \in \Re^3$ represents the angular velocity, $m \in \Re^1$ is the known mass of the quad-rotor, $J \in \Re^{3x3}$ denotes a positive definite inertia matrix, $G(R) \in \Re^3$ is a gravity vector described below, and $N_1(v)$, $N_2(\omega) \in \Re^3$ are the nonlinear aerodynamic damping interactions. The input $u_1(t) \in \Re^1$ provides lifting force in the z-direction and $u_2(t) \in \Re^3$ creates rotation torque in the roll, pitch, and yaw directions. The specific form of the quad-rotor links the inputs to the dynamics via $B_1 = [0, 0, 1]^T \in \Re^3$ and $B_2 = I_3 \in \Re^{3x3}$. Additionally, I_3 is a 3x3 identity matrix, $O_{3x1} \in \Re^3$ represents a 3x1 zero vector and $O_{3x3} \in \Re^{3x3}$ represents a 3x3 zero matrix, and $S(\cdot) \in \Re^{3x3}$ is a general form of skew-symmetric matrix as follows

$$S(\xi) = \begin{bmatrix} 0 & -\xi_3 & \xi_2 \\ \xi_3 & 0 & -\xi_1 \\ -\xi_2 & \xi_1 & 0 \end{bmatrix}, \quad \xi = [\xi_1, \xi_2, \xi_3]^T \in \Re^{3x1}. \tag{2}$$

It will be necessary to relate the inertial frame coordinates to the body-fixed frame coordinates as seen in Figure 1. The quaternion based rotation matrix $R(q) \in \Re^{3x3}$ that translates a body-fixed frame vector into inertial coordinates is calculated from the following form

$$R(q) = (q_o^2 - q_v^T q_v) I_3 + 2 q_v q_v^T - 2 q_o S(q_v) \tag{3}$$

where $q(t) = [q_o, q_v^T]^T \in \Re^4$ represents the unit quaternion, $q_o(t) \in \Re^1$, $q_v(t) \in \Re^3$ are subject to the constraint $q_o^2 + q_v^T q_v = 1$ [11]. The unit quaternion can be generated from $\omega(t)$ by the relationship [12]

$$\dot{q}(t) = \begin{bmatrix} \dot{q}_o \\ \dot{q}_v \end{bmatrix} = \begin{bmatrix} -\frac{1}{2} q_v^T \\ \frac{1}{2}(S(q_v) + q_o I_3) \end{bmatrix} \omega. \tag{4}$$

The angular velocity transformation matrix based on the Euler angles [12], denoted as

$$T(\Theta) = \begin{bmatrix} T_x(\Theta) \\ T_y(\Theta) \\ T_z(\Theta) \end{bmatrix} = \begin{bmatrix} 1 & s\phi t\theta & c\phi t\theta \\ 0 & c\phi & -s\phi \\ 0 & \frac{s\phi}{c\theta} & \frac{c\phi}{c\theta} \end{bmatrix} \in \Re^{3x3}, \tag{5}$$

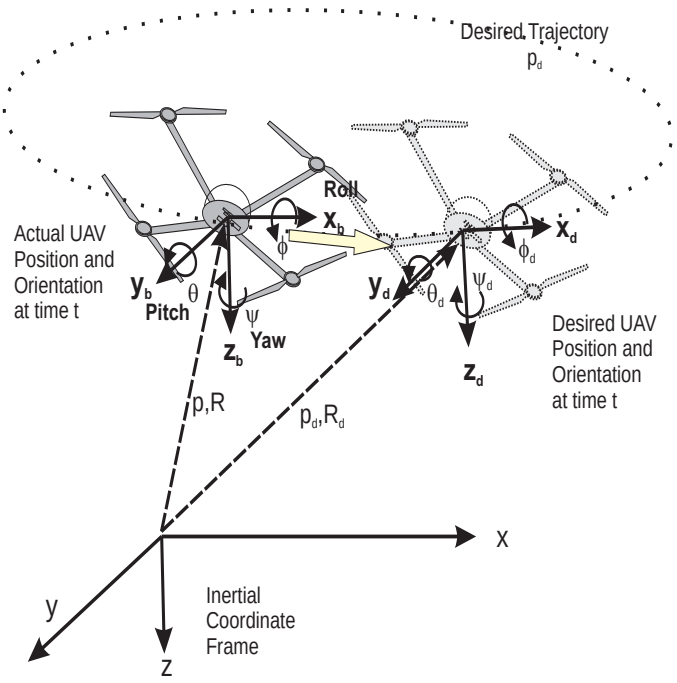

Figure 1: Quad-Rotor UAV Coordinates

is used to relate the rate of change to the angular velocities in the body-fixed frame by the following expression

$$\dot{\Theta} = T(\Theta)\omega \tag{6}$$

where the Euler angles, $\Theta(t) = [\phi, \theta, \psi]^T \in \Re^3$, describe the orientation of the body-fixed frame relative to the inertial frame and in which $c\cdot = cos\,(\cdot)$, $s\cdot = sin\,(\cdot)$, $t\cdot = tan\,(\cdot)$ are used. Note that we use the quaternion based translational rotation matrix, $R(q)$, in order to avoid the matrix singularity associated with the Euler angles representation where possible; however, the Euler angles based angular transformation matrix must be used to facilitate access to the yaw angle for tracking control. A gravity vector is denoted as

$$G(R) = mgR^T(q)E_z \in \Re^3 \tag{7}$$

where $g \in \Re^1$ denotes the gravitational acceleration due to the gravity and $E_z = [0, 0, 1]^T$ denotes the unit vector in the coordinates of the inertial frame. $G(R)$ is represented in the body-fixed frame as the multiplication by $R^T(q)$ would indicate.

The translational and rotational kinematic equations in the body-fixed reference frame are given by

$$\begin{bmatrix} v \\ \omega \end{bmatrix} = \begin{bmatrix} R^T(q) & O_{3x3} \\ O_{3x3} & T^{-1}(\Theta) \end{bmatrix} \begin{bmatrix} \dot{p} \\ \dot{\Theta} \end{bmatrix} \tag{8}$$

where $p(t) \in \Re^3$ contains the position of the body-fixed reference frame relative to the inertial frame, and its derivative $\dot{p}(t) \in \Re^3$ represents the translational velocity in the inertial frame. The transformation in (8) can be reduced to the simplified form

$$\Phi(v, \omega) = D(R, T)\dot{x} \tag{9}$$

where

$$\Phi(v, \omega) \triangleq [v^T, \omega^T]^T \in \Re^6,\ x \triangleq [p^T, \Theta^T]^T \in \Re^6, \tag{10}$$

and

$$D(R,T) \triangleq \begin{bmatrix} R^T(q) & O_{3x3} \\ O_{3x3} & T^{-1}(\Theta) \end{bmatrix} \in \Re^{6x6}. \tag{11}$$

The dynamics in (1) can be compacted and transformed into the inertial frame as shown in Appendix A to yield the dynamic model

$$M^*(R,T)\ddot{x} = N^*(R,T,\dot{x})\dot{x} + h^*(R,T,\dot{x}) + G^*(R) + B^*(R,T)\bar{U} \tag{12}$$

where $M^*(R,T) \in \Re^{6x6}$ denotes the inertia matrix, $N^*(R,T,\dot{x}) \in \Re^{6x6}$ is a Centrifugal/Coriolis force matrix, $h^*(R,T,\dot{x}) \in \Re^6$ is a hydrodynamic damping term, $G^*(R) \in \Re^6$ is a gravity term, and $B^*(R,T) \in \Re^{6x4}$ represents the input matrix. All are explicitly defined as (143) in Appendix A.

2.2 Model Properties and Assumptions

2.2.1 Model Properties

The dynamic system given in (12) satisfies the following properties.

P1: The inertia matrix $M^*(R,T)$ and Centrifugal/Coriolis matrix $N^*(R,T,\dot{x})$ in (12) satisfy the following skew-symmetric property [9]

$$\xi^T \left(\frac{d}{dt}\left(M^*(R,T)\right) + 2N^*(R,T,\dot{x}) \right) \xi = 0, \ \forall\ \xi \in \Re^6,$$

which is proven in Appendix B.

P2: The inertia matrix $M^*(R,T)$ can be upper and lower bounded in the following form

$$m_1 \left\|\xi\right\|^2 \leq \xi^T M^*(R,T)\xi \leq m_2 \left\|\xi\right\|^2, \ \forall\ \xi \in \Re^6$$

where m_1, $m_2 \in \Re^1$ are positive constants.

The rotation matrix $R(q)$ of (3) where $R(q) = R(\Theta)$ and the skew-symmetric matrix $S(\omega)$ of (2) satisfy the following properties [12].

P3: $\dot{R} = RS(\omega)$, $\dot{R}^T = -S(\omega)R^T$

P4: $R^T = R^{-1}$, $R^TR = RR^T = I_3$

P5: $S^T(\xi) = -S(\xi)$, $S(\xi)\delta = -S(\delta)\xi$, $\forall \xi, \delta \in \Re^3$

2.2.2 Model Assumptions

The following assumptions are made regarding specific components of the dynamic model. Note that this assumptions can be shown true for specific models but not in general.

A1: With regard to angular transformation matrix, $T(\Theta)$ introduced in (5), we assume that $\theta \neq \pm\frac{\pi}{2}$ or $T^{-1}(\Theta)$ exists and $\left\|T(\Theta)\right\|_{i_\infty}$ is bounded (i.e., $\left\|T(\Theta)\right\|_{i_\infty} \leq \varepsilon_1$ where $\varepsilon_1 \in \Re^1$ is a positive constant).

A2: The nonlinear damping term $N_1(v) \in \Re^3$, $N_2(\omega) \in \Re^3$ introduced in (1) can be replaced by the linearly parameterized form $Y_1(v)\theta_1 = N_1(v)$, $Y_2(\omega)\theta_2 = N_2(\omega)$ where $Y_1(v) \in \Re^{3xl}$, $Y_2(\omega) \in \Re^{3xm}$ are known regression matrices and $\theta_1 \in \Re^l$, $\theta_2 \in \Re^m$ are known parameter vectors. The dimension of l and m are related to the specific model for $N_1(v)$, $N_2(\omega)$. Additionally, it is assumed that the first nonlinear parameterized term can be upper bounded as

$$\|Y_1(v)\theta_1\| \leq \xi_{c4} \|v\|, \text{ where } \xi_{c4} \in \Re^1 \text{ is a positive constnat.}$$

A3: The nonlinear term $h^*(\cdot) \in \Re^6$ in (12) can be linearly parameterized in terms of $\dot{x}(t)$ as follows

$$h^*(R, T, \dot{x}) \triangleq Y^*(R, T)\dot{x} \tag{13}$$

in which $Y^*(R, T) \in \Re^{6xp}$ and $Y^*(R, T)$ can be upper bounded in the following form

$$\|Y^*(R, T)\| \leq \xi_{c0}, \text{ where } \xi_{c0} \in \Re^1 \text{ is a positive constant.} \tag{14}$$

3 Output Feedback Tracking Control

The goal of the tracking controller is to force the aerial vehicle track a desired trajectory. As discussed in the modeling section, the quad-rotor aerial vehicle is under-actuated, and hence, a decision must be made as to which degrees of freedom are to be controlled. First the choice was made to control the translational position, $p(t) \in \Re^3$ in the inertial reference frame, along with yaw, $\psi(t) \in \Re^1$ in the inertial reference frame. The translational position $p(t)$ and the angular position $\Theta(t) \in \Re^3$ are the only measurable states, other states such as the translational velocity $v(t) \in \Re^3$ and the angular velocity $\omega(t) \in \Re^3$ are not measurable and cannot be included in the controller design. Here we assume that the desired trajectories and their up to third derivatives are all bounded; i.e., $p_d(t)$, $\dot{p}_d(t)$, $\ddot{p}_d(t)$, and $\dddot{p}_d(t) \in \mathcal{L}_\infty$ and $\psi_d(t), \dot{\psi}_d(t)$, and $\ddot{\psi}_d(t) \in \mathcal{L}_\infty$.

3.0.3 Full State Feedback (FSFB) Error Systems to Motivate the Structure of the Output Feedback Control

In order to demonstrate the approach to designing an OFB controller the same approach is demonstrated for the less complicated FSFB. The position tracking error, denoted as $e_p(t) \in \Re^3$, expressed in the body-fixed frame is defined as the transformed difference between the inertial-frame based position and the inertial-frame based desired position, denoted as $p_d(t) \in \Re^3$, in the manner

$$e_p \triangleq R^T(p - p_d). \tag{15}$$

The position tracking error rate, $\dot{e}_p(t) \in \Re^3$, is obtained by taking the time derivative of (15),

$$\dot{e}_p = \dot{R}^T(p - p_d) + R^T\dot{p} - R^T\dot{p}_d, \tag{16}$$

and after substituting for $\dot{R}^T = -S(\omega)R^T$ from P3, and $\dot{p}(t) = Rv$ from (8), and using $R^TR = I_3$ in P4 we have

$$\dot{e}_p = -S(\omega)R^T(p - p_d) + v - R^T\dot{p}_d. \tag{17}$$

We now use the definition of $e_p(t)$ in (15) to collect terms in (17) and then the term $\frac{1}{m}R^T\dot{p}_d(t)$ is added and subtracted to facilitate the introduction of the term $e_v(t) \in \Re^3$ as follows

$$\dot{e}_p = -S(\omega)e_p + \frac{1}{m}(mv - R^T\dot{p}_d) + \frac{1}{m}R^T\dot{p}_d - R^T\dot{p}_d. \tag{18}$$

From the equation in (18) the translational velocity tracking error, $e_v(t) \in \Re^3$, in the body-fixed frame is defined as

$$e_v \triangleq mv - R^T \dot{p}_d \tag{19}$$

where $\dot{p}_d(t) \in \Re^3$ is the desired translational velocity. The final form of the open-loop position tracking error dynamics in full state feedback system is obtained from (18), (19) as follows

$$\dot{e}_p = -S(\omega)e_p + \frac{1}{m}e_v + (\frac{1}{m} - 1)R^T \dot{p}_d. \tag{20}$$

After taking the time derivative of $e_v(t)$ in (19), then substituting for $m\dot{v}(t)$ from (1) and for $\dot{R}^T(\cdot) = -S(\omega)R^T$ from P3, we have

$$\dot{e}_v = -mS(\omega)v + Y_1(v)\theta_1 + G(R) + B_1 u_1 + S(\omega)R^T \dot{p}_d - R^T \ddot{p}_d \tag{21}$$

where A2 was used to replace $N_1(v)$. After collecting the terms in (21) and applying the $e_v(t)$ definition in (19), we have the velocity error rate as

$$\dot{e}_v = -S(\omega)e_v + G(R) + Y_1(v)\theta_1 - R^T \ddot{p}_d + B_1 u_1. \tag{22}$$

The yaw angle tracking error, $e_\psi(t) \in \Re^1$, is defined in the inertial coordinate system as

$$e_\psi \triangleq \psi - \psi_d. \tag{23}$$

The goal in the control development will be to ensure that $e_\psi(t)$ and $e_p(t)$ are driven to small values; that is, to ensure the control objectives are met. The yaw angle rate error system is derived by taking the time derivative of (23) as follows

$$\dot{e}_\psi = \dot{\psi} - \dot{\psi}_d = T_z(\Theta)\omega - \omega_{zd} \tag{24}$$

where the term $T_z(\Theta) \in \Re^{1x3}$ is the third row of $T(\Theta)$ from (5). Note that $T_z(\Theta)\omega = \dot{\psi}$ in (6) and $\omega_{zd} = \dot{\psi}_d$ where $\omega_{zd}(t)$ is the desired yaw angle rate in the body-fixed frame. In order to further develop the control design, the filtered position tracking error signal $r_p(t) \in \Re^3$ is defined in the following manner [6]

$$r_p \triangleq e_v + \alpha e_p + \delta \tag{25}$$

where $\alpha \in \Re^1$ is a positive constant and $\delta = \begin{bmatrix} 0 & 0 & \delta_3 \end{bmatrix}^T \in \Re^3$ is a constant design vector in which $\delta_3 \in \Re^1$ is a scalar constant. The filtered position tracking error can be combined with the yaw tracking error to create a composite tracking error $r(t) \in \Re^4$ in the manner

$$r = \begin{bmatrix} r_p \\ e_\psi \end{bmatrix}. \tag{26}$$

The filtered tracking error dynamics can be found by first differentiating (26) to yield

$$\dot{r} = \begin{bmatrix} \dot{r}_p \\ \dot{e}_\psi \end{bmatrix} = \begin{bmatrix} \dot{e}_v + \alpha \dot{e}_p \\ \dot{e}_\psi \end{bmatrix}. \tag{27}$$

The filtered position tracking error rate, $\dot{r}_p(t)$, are obtained by substituting (20) and (22) to yield

$$\dot{r}_p = -S(\omega)(e_v + \alpha e_p + \delta - \delta) + \frac{\alpha}{m}e_v + \alpha(\frac{1}{m} - 1)R^T \dot{p}_d - R^T \ddot{p}_d + G(R) + Y_1(v)\theta_1 + B_1 u_1 \tag{28}$$

where the term $S(\omega)\delta$ has been added and subtracted to facilitate introduction of $\dot{r}_p(t) \in \Re^3$ on the right-hand side as shown below

$$\dot{r}_p = -S(\omega)r_p + \frac{\alpha}{m}e_v + \alpha(\frac{1}{m} - 1)R^T\dot{p}_d - R^T\ddot{p}_d + G(R) + Y_1(v)\theta_1 + [S(\omega)\delta + B_1u_1]\,. \tag{29}$$

It is now a straightforward matter to substitute from (24) and (29) into (27) to yield the open-loop filtered tracking error dynamics in the following form

$$\dot{r} = \begin{bmatrix} -S(\omega)r_p + \frac{\alpha}{m}e_v + \alpha(\frac{1}{m} - 1)R^T\dot{p}_d - R^T\ddot{p}_d + G(R) + Y_1(v)\theta_1 \\ -\omega_{zd} \end{bmatrix} + \begin{bmatrix} -S(\delta)\omega + B_1u_1 \\ T_z(\Theta)\omega \end{bmatrix} \tag{30}$$

where $S(\xi)\delta = -S(\delta)\xi$ in P5 was used to modify the $S(\omega)\delta$ term. The last square bracketed term in (30) highlights the location where the control input will be eventually designed. The control input, $u_1(t)$ can be designed by introducing the auxiliary signal $z(t) \in \Re^3$ in order to inject an auxiliary control signal $\bar{u}_1(t)$ into the translational dynamics from the rotational dynamics, $\omega(t)$ as

$$z = \omega - B_z\bar{u}_1 \tag{31}$$

where $B_z = [I_3, O_{3\text{x}1}] \in \Re^{3\text{x}4}$ and the control input is defined by

$$u_1 = \begin{bmatrix} 0 & 0 & 0 & 1 \end{bmatrix} \bar{u}_1 \tag{32}$$

Then we have

$$\dot{r} = \begin{bmatrix} -S(\omega)r_p + \frac{\alpha}{m}e_v + \alpha(\frac{1}{m} - 1)R^T\dot{p}_d - R^T\ddot{p}_d + G(R) + Y_1(v)\theta_1 + \frac{1}{m}(e_p - e_p) \\ -\omega_{zd} \end{bmatrix} + B_\mu\bar{u}_1 + B_\mu\begin{bmatrix} z \\ 0 \end{bmatrix} \tag{33}$$

where the procedure is detailed in the Appendix C titled "Development and Derivative of Control Signal $\bar{u}_1(t)$", the term $\frac{1}{m}e_p(t)$ was added and subtracted in (30) to facilitate further control development, and $B_\mu(\cdot) \in \Re^{4\text{x}4}$ is defined as

$$B_\mu = \begin{bmatrix} -S(\delta) & B_1 \\ T_z(\Theta) & 0 \end{bmatrix}. \tag{34}$$

3.1 Observer Design

The next step in the control development is to address the problem that the velocity of the aerial vehicle, $\dot{x}(t)$ is not directly measurable. In the inertial coordinate system the vehicle velocity and vehicle angular velocity, $\dot{x}(t)$, cannot be obtained from sensor readings. The well known method of circumventing this problem is to create an estimate of the unmeasurable states for use in the feedback control law. The estimated linear and angular velocities $\hat{v}(t)$, $\hat{\omega}(t) \in \Re^3$ are introduced using (9) as

$$\begin{bmatrix} \hat{v} \\ \hat{\omega} \end{bmatrix} = \begin{bmatrix} R^T(q) & O_{3\text{x}3} \\ O_{3\text{x}3} & T^{-1}(\Theta) \end{bmatrix} \begin{bmatrix} \dot{\hat{p}} \\ \dot{\hat{\Theta}} \end{bmatrix}. \tag{35}$$

The equation (35) can be rewritten by introducing $\hat{\Phi}(\hat{v}, \hat{\omega}) = [\hat{v}^T, \hat{\omega}^T]^T \in \Re^6$ and $\dot{\hat{x}}\ (t) = [\dot{\hat{p}}^T, \dot{\hat{\Theta}}^T]^T$ to yield

$$\hat{\Phi}(\hat{v}, \hat{\omega}) = D(R, T)\ \dot{\hat{x}}\ . \tag{36}$$

The goal of estimating velocity is achieved by using an observer similar to [9] as follows

$$\dot{\hat{x}} = y + k_{01}\tilde{x} \tag{37}$$

where the initial condition $y(0) = -k_{01}\tilde{x}(0)$, $k_{01} \in \Re^1$ is a positive gain and $\tilde{x}(t) = [\tilde{p}^T, \tilde{\Theta}^T] \in \Re^6$ is defined as

$$\tilde{x} = x - \hat{x} \tag{38}$$

where $\hat{x}(t) = [\hat{p}^T, \hat{\Theta}^T]^T \in \Re^6$ denotes a position estimate vector. The auxiliary signal $y(t) \in \Re^6$ introduced in (37) is updated according to

$$\dot{y} = M^*(R,T)^{-1}\left(N^*(R,T,\dot{x}_o)\dot{x}_o + h^*(R,T,\dot{x}_o) + G^*(R) + B^*(R,T)\bar{U} + k_{02}\tilde{x}\right) + \overline{k}_{03}\tilde{x} \tag{39}$$

where k_{02}, $\overline{k}_{03} \in \Re^1$ are positive constants and an auxiliary signal $\dot{x}_o(t) \in \Re^6$ is defined as

$$\dot{x}_o = \dot{\hat{x}} - \beta\tilde{x} \tag{40}$$

where $\beta \in \Re^1$ is a positive constant. The equation (39) was obtained by substituting $\dot{x}_o(t)$ for $\dot{x}(t)$ into the dynamic model in (12) and adding the $\tilde{x}$-terms to promote stability of the observer. The basic form of the internal observer signal $\dot{y}(t) \in \Re^6$ comes from substituting $\dot{x}_o(t)$ into the modeling equation of (12); that is, the knowledge of the system dynamics and parameters are exploited to produce the velocity estimate. In order to simplify the Lyapunov analysis, the following filtered observer error signal is defined simlar to [10] as

$$s \triangleq \dot{x} - \dot{x}_o = \dot{\tilde{x}} + \beta\tilde{x} \in \Re^6 \tag{41}$$

where (40) was used. This estimate must be faithful to the actual velocity signal in the sense that the velocity estimate, $\dot{\hat{x}}\ (t)$, will produce a small value for the velocity estimation error, $\dot{\tilde{x}}\ (t) \in \Re^6$, defined as

$$\dot{\tilde{x}} = \dot{x} - \dot{\hat{x}} \tag{42}$$

where the estimated velocity errors can be represented by defining

$$\tilde{\Phi}(\tilde{v}, \tilde{\omega}) = \begin{bmatrix} \tilde{v} \\ \tilde{\omega} \end{bmatrix} \triangleq D(R,T)\ \dot{\tilde{x}} = D(R,T) \begin{bmatrix} \dot{\tilde{p}} \\ \dot{\tilde{\Theta}} \end{bmatrix} \tag{43}$$

and

$$\dot{\tilde{p}} = \dot{p} - \dot{\hat{p}} \ \text{ and } \ \dot{\tilde{\Theta}} = \dot{\Theta} - \dot{\hat{\Theta}}\ . \tag{44}$$

The motivation for the form of the observer and the proof that the observer will produce a proper estimate in the observation error dynamics is developed below. Taking the time derivative of (37) yields

$$\ddot{\hat{x}} = \dot{y} + k_{01}\ \dot{\tilde{x}}\ . \tag{45}$$

Multiplying (45) by $M^*(R,T)$, and then substituting from (39) for $M^*(R,T)\dot{y}(t)$ yields

$$\begin{aligned} M^*(R,T)\ \ddot{\hat{x}} \ &= \ N^*(R,T,\dot{x}_o)\dot{x}_o + h^*(R,T,\dot{x}_o) + G^*(R) + B^*(R,T)\bar{U} \\ &\quad + k_{02}\tilde{x} + \overline{k}_{03}M^*(R,T)\tilde{x} + k_{01}M^*(R,T)\ \dot{\tilde{x}}\ . \end{aligned} \tag{46}$$

After subtracting (46) from (12), the dynamics of $\tilde{x}(t)$ is as follows

$$\begin{aligned} M^*(R,T)\,\ddot{\tilde{x}} &= N^*(R,T,\dot{x})\dot{x} - N^*(R,T,\dot{x}_o)\dot{x}_o + h^*(R,T,\dot{x}) - h^*(R,T,\dot{x}_o) \\ &\quad -k_{02}\tilde{x} - \overline{k}_{03}M^*(R,T)\tilde{x} - k_{01}M^*(R,T)\,\dot{\tilde{x}}\,. \end{aligned} \tag{47}$$

On the other hand, taking time derivative of (41), and multiplying $M^*(R,T)$ yields

$$M^*(R,T)\dot{s} = M^*(R,T)\,\ddot{\tilde{x}} + \beta M^*(R,T)\,\dot{\tilde{x}}\,. \tag{48}$$

Substituting (47) for $M^*(R,T)\,\ddot{\tilde{x}}\,(t)$ and arranging the terms yields

$$\begin{aligned} M^*(R,T)\dot{s} &= N^*(R,T,\dot{x})\dot{x} - N^*(R,T,\dot{x}_o)\dot{x}_o + h^*(R,T,\dot{x}) - h^*(R,T,\dot{x}_o) \\ &\quad -[k_{02} + \overline{k}_{03}M^*(R,T)]\tilde{x} + [\beta - k_{01}]M^*(R,T)\,\dot{\tilde{x}}\,. \end{aligned} \tag{49}$$

Introducing the new positive constants

$$\overline{k}_{03} = k_{03}\beta \text{ and } k_{01} = \beta + k_{03} \tag{50}$$

allows the last two terms in the right side of the (49) to be rewritten as

$$\begin{aligned} M^*(R,T)\dot{s} &= N^*(R,T,\dot{x})\dot{x} - N^*(R,T,\dot{x}_o)\dot{x}_o + h^*(R,T,\dot{x}) - h^*(R,T,\dot{x}_o) \\ &\quad -k_{02}\tilde{x} - k_{03}M^*(R,T)s \end{aligned} \tag{51}$$

where (41) was used. The definition of $s(t)$ in (41) is substituted as $\dot{x}(t) = s(t) + \dot{x}_o(t)$ into the outside term of the first equation to the right side in (51) and then, we have

$$\begin{aligned} M^*(R,T)\dot{s} &= N^*(R,T,\dot{x})s + N^*(R,T,\dot{x})\dot{x}_o - N^*(R,T,\dot{x}_o)\dot{x}_o + h^*(R,T,\dot{x}) - h^*(R,T,\dot{x}_o) \\ &\quad -k_{02}\tilde{x} - k_{03}M^*(R,T)s. \end{aligned} \tag{52}$$

Substituting A3 yields

$$M^*(R,T)\dot{s} = N^*(R,T,\dot{x})s + N^*(R,T,\dot{x})\dot{x}_o - N^*(R,T,\dot{x}_o)\dot{x}_o + Y^*(R,T)s - k_{02}\tilde{x} - k_{03}M^*(R,T)s. \tag{53}$$

The Centrifugal/Coriolis terms, $N^*(R,T,\dot{x})\dot{x}_o - N^*(R,T,\dot{x}_o)\dot{x}_o$ are now utilized to write $N_c^*(R,T,\dot{x}_o)s$ developed in the Appendix F. Therefore, the velocity observer error dynamics yields

$$M^*(R,T)\dot{s} = N^*(R,T,\dot{x})s + N_c^*(R,T,\dot{x}_o)s + Y^*(R,T)s - k_{02}\tilde{x} - k_{03}M^*(R,T)s \tag{54}$$

3.2 Output Feedback Control Formulation

Figure 2 shows the outline of the output feedback tracking system. We designed the observer to estimate the velocities $v(t)$, $\omega(t)$ which are not measurable, producing $\dot{\hat{x}}\,(t)$ and then closed-loop controller using backstepping approach based on the Lyapunov stability which will enable to track the desired position and yaw angle is designed using the output feedback and estimated states based on the error dynamics of the underactuated UAV system.

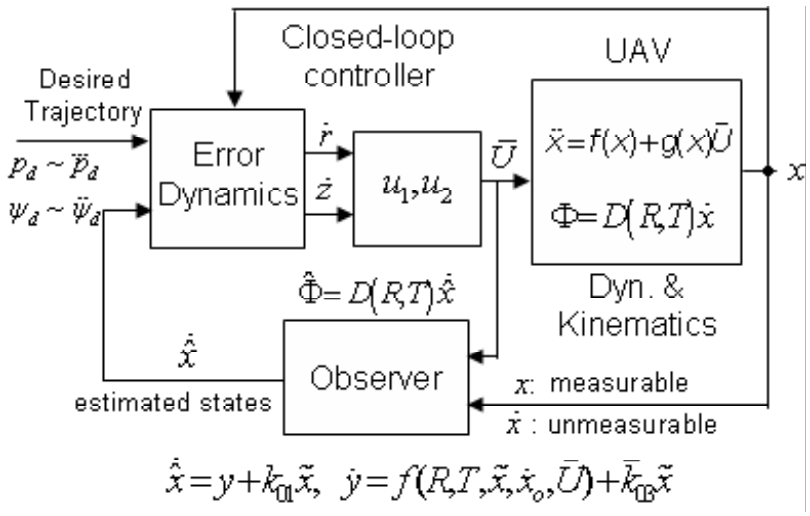

Figure 2: Block Diagram of OFB Position and Yaw Tracking System

3.2.1 Error Definition in Output Feedback Control

In the OFB only the position tracking error in (15) and yaw angle tracking error in (19) are same those of full state feedback system. The definition of velocity tracking error in (19) is now used as a guide to account for the fact that the velocity is not measurable. Specifically, an observed velocity tracking error signal, $\hat{e}_v(t) \in \Re^3$, can be defined by substituting the estimated linear velocity, $\hat{v}(t)$, into (19) as

$$\hat{e}_v \triangleq m\hat{v} - R^T \dot{p}_d. \tag{55}$$

The velocity error rate equation in (22) is redefined by substituting $\hat{v}(t)$ and $\hat{\omega}(t)$ to yield the observed vlocity rate error as

$$\dot{\hat{e}}_v = -S(\hat{\omega})\hat{e}_v + G(R) + Y_1(\hat{v})\theta_1 - R^T \ddot{p}_d + B_1 u_1. \tag{56}$$

In a similar fashion, $\dot{\hat{e}}_p(t)$ can be formed from (20) by substituting $\hat{\omega}$ and $\hat{e}_v$

$$\dot{\hat{e}}_p = -S(\hat{\omega})e_p + \frac{1}{m}\hat{e}_v + (\frac{1}{m} - 1)R^T \dot{p}_d. \tag{57}$$

The new signal $\hat{r}(t) \in \Re^4$ has been introduced to represent the observed filtered tracking error and is defined by

$$\hat{r} = \begin{bmatrix} \hat{r}_p \\ e_\psi \end{bmatrix} = \begin{bmatrix} \hat{e}_v + \alpha e_p + \delta \\ \psi - \psi_d \end{bmatrix}. \tag{58}$$

The component definition of $\hat{r}(t)$ in (58) can be differentiated to yield

$$\dot{\hat{r}} = \begin{bmatrix} \dot{\hat{r}}_p \\ \dot{\hat{e}}_\psi \end{bmatrix} = \begin{bmatrix} \dot{\hat{e}}_v + \alpha \dot{\hat{e}}_p \\ \dot{\psi} - \dot{\psi}_d \end{bmatrix}. \tag{59}$$

The observed filtered position error rate, $\dot{\hat{r}}_p(t)$ is found by substituting (56) and (57) into the top row of (59) to yield

$$\dot{\hat{r}}_p = -S(\hat{\omega})\hat{r}_p + \frac{\alpha}{m}\hat{e}_v + \alpha(\frac{1}{m} - 1)R^T \dot{p}_d + G(R) + Y_1(\hat{v})\theta_1 - R^T \ddot{p}_d + [-S(\delta)\hat{\omega} + B_1 u_1]. \tag{60}$$

The rate of yaw error is found by substituting $\hat{\omega}(t)$ into (24)

$$\dot{\hat{e}}_{\psi}=\dot{\hat{\psi}} -\omega_{zd} = T_z(\Theta)\hat{\omega} - \omega_{zd} \tag{61}$$

where $\dot{\psi}_d(t) = \omega_{zd}$. The observed tracking error rate is obtained by substituting (60) and (61) as

$$\dot{\hat{r}}= \begin{bmatrix} S(\hat{\omega})\hat{r}_p + \frac{\alpha}{m}\hat{e}_v + \alpha(\frac{1}{m}-1)R^T\dot{p}_d + G(R) + Y_1(\hat{v})\theta_1 - R^T\ddot{p}_d \\ -\omega_{zd} \end{bmatrix} + \begin{bmatrix} -S(\delta)\hat{\omega} + B_1u_1 \\ T_z(\Theta)\hat{\omega} \end{bmatrix}. \tag{62}$$

The equation (62) can be derived by following the procedure which is shown the equations from (30) to (34) as

$$\dot{\hat{r}}= \begin{bmatrix} -S(\hat{\omega})\hat{r}_p + \frac{\alpha}{m}\hat{e}_v + \alpha(\frac{1}{m}-1)R^T\dot{p}_d + G(R) + Y_1(\hat{v})\theta_1 - R^T\ddot{p}_d \\ -\omega_{zd} \end{bmatrix} + B_{\mu}\bar{u}_1 + B_{\mu}\begin{bmatrix} \hat{z} \\ 0 \end{bmatrix} \tag{63}$$

where the auxiliary signal $\hat{z}(t) \in \Re^3$ is introduced in the same way in (31) by substituting $\hat{\omega}(t)$ to denote

$$\hat{z} = \hat{\omega} - B_z\bar{u}_1, \tag{64}$$

and hence, the auxiliary estimation signal $\tilde{z}(t) \in \Re^3$ can be defined using the (31) and (64) as

$$\tilde{z} = \omega - \hat{\omega} = \tilde{\omega}. \tag{65}$$

3.3 Controller Formulation

3.3.1 Translational Input as a Lifting force

The filtered tracking error dynamics in (33) now presents the opportunity to design the auxiliary control input $\bar{u}_1(t)$. It can be seen from (33) that certain terms, those containing measurable signals, can be directly canceled by design of $\bar{u}_1(t)$. Other unmeasurable terms, e.g., $e_v(t)$, $r_p(t)$, $Y_1(v)\theta_1$, can be canceled to the best degree possible using an estimate of velocity. Additionally, a term of the form $-r(t) \in \Re^4$ will be required to promote the convergence of $r(t)$ to zero. With these three objectives in mind, the control $\bar{u}_1(t)$ in (33) can be designed based on equation (63) as

$$\bar{u}_1 = B_{\mu}^{-1}\left(-k_r\hat{r} + \begin{bmatrix} -\frac{\alpha}{m}\hat{e}_v - \alpha(\frac{1}{m}-1)R^T\dot{p}_d - G(R) - Y_1(\hat{v})\theta_1 + R^T\ddot{p}_d - \frac{1}{m}e_p \\ \omega_{zd} \end{bmatrix}\right) \tag{66}$$

where k_r =diag$(k_{r1}, k_{r1}, k_{r1}, k_{r2}) \in \Re^{4x4}$ is a positive constant matrix. For stability analysis of this control, the observed filtered tracking error, denoted by $\tilde{r}(t) \in \Re^4$, can be described by subtracting (58) from (26) as

$$\tilde{r} = r - \hat{r} = \begin{bmatrix} r_p - \hat{r}_p \\ 0 \end{bmatrix} = \begin{bmatrix} \tilde{r}_p \\ 0 \end{bmatrix} \tag{67}$$

where the observed filtered position tracking estimation error, $\tilde{r}_p(t) \in \Re^3$ is now defined as the difference between $r_p(t)$ in (25) and $\hat{r}_p(t)$ in (58) and can be shown to be

$$\tilde{r}_p = r_p - \hat{r}_p = m\tilde{v}. \tag{68}$$

The difference between the actual velocity error, $e_v(t)$, and the estimated velocity error, $\hat{e}_v(t)$ is defined as

$$\tilde{e}_v = e_v - \hat{e}_v = m(v - \hat{v}) = m\tilde{v} = \tilde{r}_p \tag{69}$$

where $\tilde{v}(t) = v - \hat{v}$ is the velocity tracking error. The equation (66) can be represented by substituting $-r(t) + \tilde{r}(t)$ for $-\hat{r}(t)$ and substituting $-e_v(t) + \tilde{e}_v(t)$ for $-\hat{e}_v(t)$ in the following form

$$\bar{u}_1 = B_\mu^{-1} \left\{ -k_r r + k_r \tilde{r} + \left[\begin{array}{c} -\frac{\alpha}{m} e_v + \frac{\alpha}{m} \tilde{e}_v - \alpha(\frac{1}{m} - 1) R^T \dot{p}_d - G(R) - Y_1(\hat{v})\theta_1 + R^T \ddot{p}_d - \frac{1}{m} e_p \\ \omega_{zd} \end{array} \right] \right\}. \tag{70}$$

Finally, the closed-loop filtered tracking error dynamics for $\dot{r}(t)$ is formed by substituting (70) into (33) to yield

$$\dot{r} = -k_r r + k_r \left[\begin{array}{c} \tilde{r}_p \\ 0 \end{array} \right] + \left[\begin{array}{c} -S(\omega) r_p - \frac{e_p}{m} \\ 0 \end{array} \right] + \left[\begin{array}{c} \frac{\alpha}{m} \tilde{e}_v + \tilde{Y}_1 \theta_1 \\ 0 \end{array} \right] + B_\mu \left[\begin{array}{c} z \\ 0 \end{array} \right] \tag{71}$$

where (67), (69), and (31) were used, and $\tilde{Y}_1(\cdot) \in \Re^{3\text{x}l}$ is introduced as follows

$$\tilde{Y}_1(\tilde{v}) = Y_1(v) - Y_1(\hat{v}). \tag{72}$$

3.3.2 Development of the Torque Input using a Backstepping Approach

Examining the meaning of the term $z(t)$ introduced in (33) should help crystallize the exposition of the control design approach and motivate the next step. The definition of $z(t)$ in (31) quantifies the closeness of the control term $\bar{u}_1(t)$ to the angular velocities $\omega(t)$, if $z(t)$ is zero then $\omega(t) = \bar{u}_1(t)$. The implication is that the effect of rewriting the input term in (33) was to inject the signal $\bar{u}_1(t)$ as a desired input to the rotational dynamics (a backstepping approach). The design now proceeds to ensure that the auxiliary signal $z(t)$ in (31) is driven to a small value. Taking the time derivative of $z(t)$ in (31) and multiplying by the inertia matrix, J, yields

$$J\dot{z} = J\dot{\omega} - JB_z \, \dot{\bar{u}}_1 \, . \tag{73}$$

Substituting the second equation of (1) for $J\dot{\omega}(t)$ into (73) produces

$$J\dot{z} = S(J\omega)\omega + N_2(\omega) + B_2 u_2 - JB_z \, \dot{\bar{u}}_1 \tag{74}$$

where it can be viewed as backstepping -$\bar{u}_1(t)$ through the integrator. It is now useful to group terms in equation (74) and invoke A2 for the parameterization of $N_2(\omega)$ as

$$J\dot{z} = \left(S(J\omega)\omega + Y_2(\omega)\theta_2 - JB_z \, \dot{\bar{u}}_1 \right) + B_2 u_2. \tag{75}$$

The following assumption is made for (75):

A4: A linear parameterization has been assumed

$$Y_3(p, R, v, \omega)\theta_3 = S(J\omega)\omega + Y_2(\omega)\theta_2 - JB_z \, \dot{\bar{u}}_1 \tag{76}$$

where $Y_3(p, R, v, \omega) \in \Re^{3\text{x}n}$ and $\theta_3 \in \Re^n$ (i.e., there are n known parameters in θ_3 and n is determined by the specific models of (76), especially $N_1(v)$, $N_2(\omega)$ and (79)).

Using the A4, (75) is rewritten as

$$J\dot{z} = Y_3(p, R, v, \omega)\theta_3 + \ B_2 u_2. \tag{77}$$

It should also be clear that ideally the control input $u_2(t)$ would be designed to stabilize the $z(t)$-dynamics and cancel $Y_3(p, R, v, \omega)\theta_3$, of course this can not be achieved directly because both of these objectives would require knowledge of unmeasurable quantities. The estimated velocities will provide the best opportunity to achieve these goals; that is, in a similar way in (77), the estimated velocities $\hat{v}(t)$ and $\hat{\omega}(t)$ are substituted into (76) to create the estimate $Y_3(p, R, \hat{v}, \hat{\omega}) \in \Re^{3xn}$ given by

$$Y_3(p, R, \hat{v}, \hat{\omega})\theta_3 = S(J\hat{\omega})\hat{\omega} + Y_2(\hat{\omega})\theta_2 - JB_z\,\dot{\bar{u}}_1 \tag{78}$$

where $Y_2(\hat{\omega})$, $Y_3(p, R, \hat{v}, \hat{\omega})$ are the estimated regression matrices. The time derivative of $\bar{u}_1(t)$ can be calculated using the error definition in (66) as follows

$$\dot{\bar{u}}_1 \triangleq \frac{d}{dt}(B_\mu^{-1})U + (B_\mu^{-1})\frac{d}{dt}U \tag{79}$$

where $U(t)$ is from the parenthetical terms on the right equation (66) and the time derivative of $U(t)$ is defined as follows

$$\begin{aligned}\frac{d}{dt}U &= -k_r\,\dot{\hat{r}} + \begin{bmatrix} -\dfrac{\alpha}{m}\,\dot{\hat{e}}_v - \dfrac{d}{dt}\left(Y_1(\hat{v})\theta_1\right) - \dfrac{1}{m}\,\dot{\hat{e}}_p \\ 0 \end{bmatrix} \\ &\quad + \begin{bmatrix} S(\hat{\omega})\left(\frac{\alpha}{m}R^T\dot{p}_d - \alpha R^T\dot{p}_d - R^T\,\ddot{p}_d + mgR^TE_z\right) - \alpha\left(1-\frac{1}{m}\right)R^T\,\ddot{p}_d + R^T\,\dddot{p}_d \\ \dot{\omega}_{zd} \end{bmatrix}\end{aligned} \tag{80}$$

where (56), (57), (63), and $\dot{G}(R) = -S(\hat{\omega})G(R)$ are utilized and the time derivative of $Y_1(\hat{v})\theta_1$ are explicitly calculated in Appendix E.

The control input $u_2(t) \in \Re^3$ is now formulated from (77), making use of (78), in the following form

$$u_2 = B_2^{-1}\left(-k_z\hat{z} - Y_3(p, R, \hat{v}, \hat{\omega})\theta_3 - \bar{B}_\mu^T\hat{r}\right) \tag{81}$$

where the first term is a linear feedback control, the last term is added to cancel a crossing term during the Lyapunov stability analysis, and $\bar{B}_\mu(\cdot) \in \Re^{4x3}$ is formed from the first three columns of $B_\mu(\cdot)$ in (34) and can be transposed as follows

$$\bar{B}_\mu^T = [-S(\delta)^T,\ T_z(\Theta)^T]. \tag{82}$$

After substituting (81) into (77), $-z(t) + \tilde{z}(t)$ for $\hat{z}(t)$, and using $\tilde{\omega}(t) = \tilde{z}(t)$ in (65), we have

$$J\dot{z} = -k_z z + k_z\tilde{\omega} + \tilde{Y}_3\theta_3 - \bar{B}_\mu^T r + \bar{B}_\mu^T\tilde{r} \tag{83}$$

where (67) was used to create the last two terms, and the regression estimation error, $\tilde{Y}_3(\cdot) \in \Re^{3xn}$, is defined as

$$\tilde{Y}_3(\tilde{v}, \tilde{\omega}) = Y_3(p, R, v, \omega) - Y_3(p, R, \hat{v}, \hat{\omega}). \tag{84}$$

$S^T(\xi) = -S(\xi)$ in P5 can be invoked to rewrite the matrix $\bar{B}_\mu^T(\cdot)$ in (82) as

$$\bar{B}_\mu^T = [S(\delta),\ T_z(\Theta)^T], \tag{85}$$

and hence, we have

$$\bar{B}_\mu^T\tilde{r} = [S(\delta),\ T_z(\Theta)^T]\begin{bmatrix} m\tilde{v} \\ 0 \end{bmatrix} = mS(\delta)\tilde{v}. \tag{86}$$

After substituting (86) into (83), we have the final form for the closed-loop system as shown below

$$J\dot{z} = -k_z z + k_z\tilde{\omega} + \tilde{Y}_3\theta_3 - \bar{B}_\mu^T r + mS(\delta)\tilde{v}. \tag{87}$$

4 Stability Analysis

The combination of velocity observer error and closed-loop error systems given by (54), (71), and (87) yields the following stability result for the velocity observation and tracking error.

Theorem 1 *The velocity observer of (37), (39), and the control law of (70), (81) ensure that the tracking error is semi-globally uniformly ultimately bounded (SGUUB) as shown below*

$$\|\eta(t)\| \leq \sqrt{\frac{\lambda_4}{\lambda_3}\|\eta(0)\|^2 \exp(-\tfrac{2\lambda_5}{\lambda_4}t) + \frac{\lambda_4\varepsilon_0^2}{\lambda_2\lambda_3\lambda_5}(1-\exp(-\tfrac{2\lambda_5}{\lambda_4}t))} \tag{88}$$

where

$$\eta \triangleq [e_p^T,\ r^T,\ z^T, s^T,\ \tilde{x}^T]^T, \tag{89}$$

and ε_0, λ_2, λ_5 *are positive constants and* λ_3, λ_4 *are positive constants given by the following form*

$$\begin{array}{l} \lambda_3 \triangleq \min\{1, m_1, k_{02}\}, \\ \lambda_4 \triangleq \max\{1, m_2, k_{02}\}, \end{array} \tag{90}$$

under the condition that

$$k_r > 3,\ k_z > 3,\ \alpha > \frac{\lambda_2}{2}m,\ k_{02} > 2\xi_{c4}\beta, \tag{91}$$

$$k_{03} > \frac{1}{m_1}\left[\xi_{c0} + 2\xi_{c4} + \xi_{c1}(\varepsilon_2+\varepsilon_7) + 5\xi_{c1}\varepsilon_8\sqrt{\frac{\lambda_4}{\lambda_3}\|\eta(0)\|^2 + \frac{\lambda_4\varepsilon_0^2}{\lambda_2\lambda_3\lambda_5}}\right] \tag{92}$$

where ξ_{c0}, ξ_{c1}, ξ_{c4} *and* ε_1 *to* ε_8 *are some positive constants. The details of subsequent stability analysis is proved in Appendix D.*

Remark 1 *According to Theorem 1 and its subsequent composite stability analysis from (116) to (129),* $V(\eta(t))$ *is bounded. From (88), if the observer and controller gains in (92) are selected to satisfy (121), it is straightforward to see that* $\eta(t) \in \mathcal{L}_\infty$*. Hence, it ensures that the* $e_p(t)$, $r(t)$, $z(t)$, $s(t)$, *and* $\tilde{x}(t)$ *are bounded. We know that all desired position and yaw angle trajectories are bounded, and that* $R(q)$ *and* $T(\Theta)$ *are bounded, thus* $D(R,T)$ *and* $G^*(R) \in \mathcal{L}_\infty$*. We can now make a conclusion that* $p(t), \psi(t), v(t) \in \mathcal{L}_\infty$ *owing to* $e_p(t), e_v(t), e_\theta(t), r_p(t) \in \mathcal{L}_\infty$*, based on the definition of (15), (19), (23), (25). Due to the boundedness of* $v(t)$*, we observe that* $\dot{p}(t)$ *in the first equation of (8) is bounded.* $\dot{\tilde{x}}\ (t)$ *is bounded in (41) because* $s(t)$, $\tilde{x}(t) \in \mathcal{L}_\infty$*, and this ensures that* $\dot{\tilde{p}}\ (t), \dot{\tilde{\Theta}}\ (t)$ $\in \mathcal{L}_\infty$ *and we know* $\dot{\hat{p}}\ (t)$ *is bounded from (42). We also know that* $\tilde{v}(t), \tilde{\omega}(t)$ *are bounded in (43), and hence,* $\tilde{e}_v(t)$, $\tilde{r}_p(t)$, $\tilde{z}(t) \in \mathcal{L}_\infty$ *from (69), (68), (65), respectively. Also, the expression for the observed velocity* $\hat{v}(t)$ *is bounded from the definition of* $\tilde{v}(t)$ *in (164). Therefore,* $\hat{e}_v(t), \hat{r}_p(t) \in \mathcal{L}_\infty$*, so we know the filtered position error* $\hat{r}(t)$ *is bounded in (58). Owing to* $v(t)$, $\hat{v}(t)$ *are bounded, the nonlinearity of the aerodynamic damping term,* $N_1(v)$, $N_1(\hat{v})$, $Y_1(v)$, $Y_1(\hat{v}), \tilde{Y}_1(\cdot)$ *are all bounded. Hence, we can state that* $\bar{u}_1(t)$ *is bounded in (70), thus the translational control input* $u_1(t) \in \mathcal{L}_\infty$ *in (32). Owing to the fact that* $\bar{u}_1(t)$ *is bounded,* $\omega(t)$ *is bounded from (31). From (65), we know that* $\hat{\omega}(t)$ *is bounded, and hence,* $\hat{z}(t) \in \mathcal{L}_\infty$ *from (64). Therefore, since* $\hat{v}(t)$, $\hat{\omega}(t)$ *have been shown to be bounded, we know that the velocity output* $\dot{\hat{x}}\ (t)$ *is bounded from (36), thus the aerodynamic damping,* $N_2(\omega)$, $N_2(\hat{\omega})$, $Y_2(\omega)$, $Y_2(\hat{\omega})$, *and* $\tilde{Y}_2(\cdot)$ *are bounded. Hence,* $\dot{x}(t)$, $\dot{x}_o(t)$ *are bounded from (42) and (40) because of* $\dot{\hat{x}}\ (t) \in \mathcal{L}_\infty$*. From the equations of (57), (56), (61) and (63), we can see that* $\dot{\hat{e}}_p\ (t)$, $\dot{\hat{e}}_v\ (t)$, $\dot{\hat{e}}_\theta\ (t)$, *and* $\dot{\hat{r}}\ (t)$ *are all bounded which can be used to show that* $\dot{\bar{u}}_1\ (t) \in \mathcal{L}_\infty$ *in*

(79), thus $Y_3\theta_3$ is bounded in (78), and consequently the torque input $u_2(t)$ is bounded from (81) using (64), (78), and (58). Thus $\dot{\hat{v}}\ (t)$, $\dot{\hat{\omega}}\ (t) \in \mathcal{L}_\infty$, in (12), $\frac{dY_1(v)}{dt} \in \mathcal{L}_\infty$ from (194), and $\dot{y}(t)$ is bounded in (39). Therefore we can conclude that all signals remain bounded in the velocity observer and the closed-loop system.

4.1 Observer Stability Analysis

In order to analyze the results of the observer, a non-negative function $V_0(t) \in \Re^1$ is defined as follows

$$V_0 = \frac{1}{2} s^T M^*(R,T) s + \frac{1}{2} k_{02} \tilde{x}^T \tilde{x}. \tag{93}$$

The time derivative of $V_0(t)$ is

$$\dot{V}_0 = \frac{1}{2} s^T \frac{d}{dt} \left(M^*(R,T) \right) s + s^T M^*(R,T) \dot{s} + k_{02} \tilde{x}^T \ \dot{\tilde{x}} \ . \tag{94}$$

Substituting (54) into the second term of (94) and then arranging the equation yields

$$\begin{aligned} \dot{V}_0 \ &= \ \frac{1}{2} s^T \left(\frac{d}{dt} \left(M^*(R,T) \right) + 2N^*(R,T,\dot{x}) \right) s + s^T N_c^*(R,T,\dot{x}_o) s + s^T Y^*(R,T) s \\ &\quad -k_{03} s^T M^*(R,T) s - k_{02} \beta \tilde{x}^T \tilde{x}. \end{aligned} \tag{95}$$

P1 is used to show that the first term in (95) is zero because of its skew-symmetric property which is validated in Appendix B, and hence, we have

$$\dot{V}_0 = -k_{03} s^T M^*(R,T) s - k_{02} \beta \tilde{x}^T \tilde{x} + s^T N_c^*(R,T,\dot{x}_o) s + s^T Y^*(R,T) s. \tag{96}$$

The term $N_c^*(R,T,\dot{x}_o)$ is a Centrifugal/Coriolis force matrix which is derived from the difference between $N^*(R,T,\dot{x})$ in the modeling equation of (12) and $N^*(R,T,\dot{x}_o)$ in the auxiliary signal $\dot{y}(t)$ in (39) of the observer design as shown in (218) in the Appendix F. Based on the structure of $N_c^*(R,T,\dot{x}_o)$ and A1 the term $N_c^*(R,T,\dot{x}_o)$ can be shown that

$$\left\| N_c^*(R,T,\dot{x}_o) \right\| \leq \xi_{c1} \left\| \dot{x}_o \right\| \ \text{ where } \xi_{c1} \in \Re^1 \text{ is a positive constant.} \tag{97}$$

According to P2, (14) in A3, and (97), (96) can be upper bounded as follows

$$\dot{V}_0 \leq -k_{03} m_1 \left\| s \right\|^2 - k_{02} \beta \left\| \tilde{x} \right\|^2 + \xi_{c1} \left\| \dot{x}_o \right\| \cdot \left\| s \right\|^2 + \xi_{c0} \left\| s \right\|^2 . \tag{98}$$

From (40), $\dot{x}_o(t)$ can be upper bounded as

$$\left\| \dot{x}_o \right\| \leq \left\| \dot{\hat{x}} \right\| + \beta \left\| \tilde{x} \right\| ; \tag{99}$$

therefore, (99) can be used to upper bound (98) uniformly as follows

$$\dot{V}_0 \leq -(k_{03} m_1 - \xi_{c0}) \left\| s \right\|^2 - k_{02} \beta \left\| \tilde{x} \right\|^2 + \xi_{c1} (\left\| \dot{\hat{x}} \right\| + \beta \left\| \tilde{x} \right\|) \left\| s \right\|^2 . \tag{100}$$

4.2 Controller Stability Analysis

In order to prove the tracking result, a non-negative function $V_1(t) \in \Re^1$ is defined as follows

$$V_1(t) = \frac{1}{2} e_p^T e_p + \frac{1}{2} r^T r + \frac{1}{2} z^T J z. \tag{101}$$

After taking the time derivative of (101), substituting from (20), (71), and (87), we have

$$\begin{aligned} \dot{V}_1 &= e_p^T \dot{e}_p + r^T \dot{r} + z^T J \dot{z} \\ &= e_p^T \left[-S(\omega) e_p + \frac{1}{m}(r_p - \alpha e_p - \delta) + (\frac{1}{m} - 1) R^T \dot{p}_d \right] \\ &\quad + r^T \left[-k_r r + k_r \begin{bmatrix} \tilde{r}_p \\ 0 \end{bmatrix} + \begin{bmatrix} -S(\omega) r_p - \frac{e_p}{m} \\ 0 \end{bmatrix} + \begin{bmatrix} \alpha \tilde{v} + \tilde{Y}_1 \theta_1 \\ 0 \end{bmatrix} + B_\mu \begin{bmatrix} z \\ 0 \end{bmatrix} \right] \\ &\quad + z^T \left[-k_z z + k_z \tilde{\omega} + \tilde{Y}_3 \theta_3 - \bar{B}_\mu^T r + m S(\delta) \tilde{v} \right] \end{aligned} \tag{102}$$

where $e_v(t) = r_p(t) - \alpha e_p - \delta$ was used for $\dot{e}_p(t)$. After collecting terms, deleting the zero terms, canceling the cross-terms, substituting $\tilde{r}_p(t)$ from (68), and using the relationship given by

$$B_\mu \begin{bmatrix} z \\ 0 \end{bmatrix} = \begin{bmatrix} -S(\delta) z \\ T_z(\Theta) z \end{bmatrix} = \begin{bmatrix} -S(\delta) \\ T_z(\Theta) \end{bmatrix} z = \bar{B}_\mu z, \tag{103}$$

the equation (102) becomes

$$\begin{aligned} \dot{V}_1 &= -k_r r^T r - k_z z^T z - \frac{\alpha}{m} e_p^T e_p - \frac{1}{m} e_p^T \delta + e_p^T (\frac{1}{m} - 1) R^T \dot{p}_d + k_r r_p^T (m \tilde{v}) \\ &\quad + r_p^T (\alpha \tilde{v} + \tilde{Y}_1 \theta_1) + k_z z^T \tilde{\omega} + z^T m S(\delta) \tilde{v} + z^T \tilde{Y}_3 \theta_3. \end{aligned} \tag{104}$$

After upper bounding the first three terms in (104) and arranging, we have

$$\begin{aligned} \dot{V}_1 &\leq -k_r \|r\|^2 - k_z \|z\|^2 - \frac{\alpha}{m} \|e_p\|^2 + e_p^T \left[(\frac{1}{m} - 1) R^T \dot{p}_d - \frac{1}{m} \delta \right] \\ &\quad + r_p^T \left[(k_r m + \alpha) \tilde{v} + \tilde{Y}_1 \theta_1 \right] + z^T \left[\tilde{Y}_3 \theta_3 + k_z \tilde{\omega} + m S(\delta) \tilde{v} \right]. \end{aligned} \tag{105}$$

The first bracket term in (105) can be upper bounded using the inequality

$$e_p^T \left[(\frac{1}{m} - 1) R^T \dot{p}_d - \frac{1}{m} \delta \right] \leq \|e_p\| \varepsilon_0 \leq \frac{1}{2} \left(\lambda_2 \|e_p\|^2 + \frac{1}{\lambda_2} \varepsilon_0^2 \right). \tag{106}$$

An upper bound for the second and third bracketed terms in (105) is now sought. The definition of $\tilde{\Phi}(\tilde{v}, \tilde{\omega})$ in (43) is upper bounded as

$$\tilde{\Phi}(\tilde{v}, \tilde{\omega}) = D(R, T) \dot{\tilde{x}} \leq \|D(R, T)\| \left\| \dot{\tilde{x}} \right\| = d_0 \left\| \dot{\tilde{x}} \right\| \tag{107}$$

where $d_0 \in \Re^1$ is a positive constant. Hence

$$\|\tilde{v}\| \leq d_0 \left\| \dot{\tilde{x}} \right\| \text{ and } \|\tilde{\omega}\| \leq d_0 \left\| \dot{\tilde{x}} \right\|. \tag{108}$$

$\tilde{Y}_1(\tilde{v})$ and $\tilde{Y}_3(\tilde{v}, \tilde{\omega})$ are bounded utilizing (72) and A3 as follows

$$\left\| \tilde{Y}_1 \theta_1 \right\| \leq \xi_{c2} \left\| \dot{\tilde{x}} \right\| \text{ and } \left\| \tilde{Y}_3 \theta_3 \right\| \leq \xi_{c3} \left\| \dot{\tilde{x}} \right\| \tag{109}$$

where ξ_{c2}, ξ_{c3}, are positive constants. From the definition of $s(t)$ in (41), $\dot{\tilde{x}}\ (t)$ can be upper bounded as

$$\begin{aligned} \left\|\dot{\tilde{x}}\right\| &\leq \|s\| + \beta \|\tilde{x}\| \qquad (110) \\ \left\|\dot{\tilde{x}}\right\|^2 &\leq 2\|s\|^2 + 2\beta^2 \|\tilde{x}\|^2 . \qquad (111) \end{aligned}$$

Upper bounds for the last two bracket terms in (105) can be expressed in the following form by utilizing (108) for $\tilde{v}(t)$ and $\tilde{\omega}(t)$, (109) for $\tilde{Y}_1\theta_1$ and $\tilde{Y}_3\theta_3$, (110) for $\left\|\dot{\tilde{x}}\right\|$, and (111) for $\left\|\dot{\tilde{x}}\right\|^2$ to produce

$$\begin{aligned} \dot{V}_1(t) \leq\ & -k_r \|r\|^2 - k_z \|z\|^2 - (\frac{\alpha}{m} - \frac{\lambda_2}{2}) \|e_p\|^2 + \frac{1}{2\lambda_2}\varepsilon_0^2. \\ & +3\|r\|^2 + \xi_{c2}^2 \left\|\dot{\tilde{x}}\right\|^2 + \alpha^2 \left\|\dot{\tilde{x}}\right\|^2 + (k_r m)^2 \left\|\dot{\tilde{x}}\right\|^2 \qquad (112) \\ & +3\|z\|^2 + \xi_{c3}^2 \left\|\dot{\tilde{x}}\right\|^2 + k_z^2 \left\|\dot{\tilde{x}}\right\|^2 + m^2 \|S(\delta)\|^2 \left\|\dot{\tilde{x}}\right\|^2 . \end{aligned}$$

After rearranging (112), we have

$$\dot{V}_1 \leq -(k_r - 3)\|r\|^2 - (k_z - 3)\|z\|^2 - (\frac{\alpha}{m} - \frac{\lambda_2}{2})\|e_p\|^2 + \xi_{c4}\left\|\dot{\tilde{x}}\right\|^2 + \frac{\varepsilon_0^2}{2\lambda_2} \qquad (113)$$

where

$$\xi_{c4} = \xi_{c2}^2 + \xi_{c3}^2 + \alpha^2 + (k_r m)^2 + k_z^2 + m^2 \|S(\delta)\|_{i\infty}^2 .$$

After using (111), (113) becomes

$$\dot{V}_1 \leq -(k_r - 3)\|r\|^2 - (k_z - 3)\|z\|^2 - (\frac{\alpha}{m} - \frac{\lambda_2}{2})\|e_p\|^2 + 2\xi_{c4}(\|s\|^2 + \beta^2\|\tilde{x}\|^2) + \frac{\varepsilon_0^2}{2\lambda_2}. \qquad (114)$$

4.3 Composite Stability Analysis

The performance of the proposed controller and observer can now be examined by combining the non-negative functions $V_0(t)$ in (93) and $V_1(t)$ in (101) as follows

$$V \triangleq V_0 + V_1 = \frac{1}{2}e_p^T e_p + \frac{1}{2}r^T r + \frac{1}{2}z^T J z + \frac{1}{2}s^T M^*(R,T)s + \frac{1}{2}k_{02}\tilde{x}^T\tilde{x}. \qquad (115)$$

The composite function $V(t)$ now has the property

$$\frac{1}{2}\lambda_3\|\eta\|^2 \leq V \leq \frac{1}{2}\lambda_4\|\eta\|^2 \qquad (116)$$

where (89) is used. After taking time derivative of (115), and utilizing the bounds on $\dot{V}_0(t)$ and $\dot{V}_1(t)$ from (100) and (114), we have

$$\begin{aligned} \dot{V} \leq\ & -(k_r - 3)\|r\|^2 - (k_z - 3)\|z\|^2 - (\frac{\alpha}{m} - \frac{\lambda_2}{2})\|e_p\|^2 - (k_{03}m_1 - \xi_{c0})\|s\|^2 \\ & -k_{02}\beta\|\tilde{x}\|^2 + \xi_{c1}\left(\left\|\dot{\hat{x}}\right\| + \beta\|\tilde{x}\|\right)\|s\|^2 + 2\xi_{c4}\|s\|^2 + 2\xi_{c4}\beta^2\|\tilde{x}\|^2 + \frac{\varepsilon_0^2}{2\lambda_2}. \qquad (117) \end{aligned}$$

We can now upper bound $\dot{V}(t)$ of (117) as follows

$$\begin{aligned}\dot{V} &\leq -(k_r-3)\|r\|^2-(k_z-3)\|z\|^2-(\frac{\alpha}{m}-\frac{\lambda_2}{2})\|e_p\|^2 \\ &\quad -\left[k_{03}m_1-\xi_{c0}-\xi_{c1}\left\|\dot{\hat{x}}\right\|-\xi_{c1}\beta\|\tilde{x}\|-2\xi_{c4}\right]\|s\|^2 \\ &\quad +(2\xi_{c4}\beta^2-k_{02}\beta)\|\tilde{x}\|^2+\frac{\varepsilon_0^2}{2\lambda_2}. \end{aligned} \tag{118}$$

$\left\|\dot{\hat{x}}\right\|$ in (118) can be upper bounded by using (190) from Appendix D and substituting (110) into (190) as follows

$$\left\|\dot{\hat{x}}\right\| \leq (2+\varepsilon_3)\|s\|+(2+\varepsilon_3)\beta\|\tilde{x}\|+\varepsilon_4\|z\|+(\varepsilon_1+\varepsilon_5)\|r\|+(\alpha\varepsilon_1+\varepsilon_6)\|e_p\|+\varepsilon_2+\varepsilon_7. \tag{119}$$

After substituting (119) into (118) and arranging, we have

$$\begin{aligned}\dot{V} &\leq -(k_r-3)\|r\|^2-(k_z-3)\|z\|^2-(\frac{\alpha}{m}-\frac{\lambda_2}{2})\|e_p\|^2-[k_{03}m_1-\xi_{c0}-2\xi_{c4}]\|s\|^2 \\ &\quad -\xi_{c1}\left((2+\varepsilon_3)\|s\|+(3+\varepsilon_3)\beta\|\tilde{x}\|+\varepsilon_4\|z\|+(\varepsilon_1+\varepsilon_5)\|r\|+(\alpha\varepsilon_1+\varepsilon_6)\|e_p\|+\varepsilon_2+\varepsilon_7\right)\|s\|^2 \\ &\quad +(2\xi_{c4}\beta^2-k_{02}\beta)\|\tilde{x}\|^2+\frac{\varepsilon_0^2}{2\lambda_2}. \end{aligned} \tag{120}$$

Utilizing (89) for the second line in (120), $\dot{V}(t)$ yields

$$\begin{aligned}\dot{V} &\leq -(k_r-3)\|r\|^2-(k_z-3)\|z\|^2-(\frac{\alpha}{m}-\frac{\lambda_2}{2})\|e_p\|^2 \\ &\quad -[k_{03}m_1-\xi_{c0}-2\xi_{c4}-\xi_{c1}(\varepsilon_2+\varepsilon_7)-5\xi_{c1}\varepsilon_8\|\eta\|]\|s\|^2 \\ &\quad -(k_{02}\beta-2\xi_{c4}\beta^2)\|\tilde{x}\|^2+\frac{\varepsilon_0^2}{2\lambda_2}. \end{aligned} \tag{121}$$

where

$$\varepsilon_8 = \max\{(2+\varepsilon_3),(3+\varepsilon_3)\beta,\varepsilon_4,(\varepsilon_1+\varepsilon_5),(\alpha\varepsilon_1+\varepsilon_6)\}, \tag{122}$$

An upper bound can be written for (121) as

$$\begin{aligned}\dot{V} &\leq -\lambda_5\left[\|r\|^2+\|z\|^2+\|e_p\|^2+\|s\|^2+\|\tilde{x}\|^2\right]+\frac{\varepsilon_0^2}{2\lambda_2} \\ &\leq -\lambda_5\|\eta\|^2+\frac{\varepsilon_0^2}{2\lambda_2} \end{aligned} \tag{123}$$

where a positive constant scalar $\lambda_5 \in \Re^1$ is given by

$$\begin{aligned}\lambda_5 &= \min\big\{(k_r-3),(k_z-3),(\tfrac{\alpha}{m}-\tfrac{\lambda_2}{2}),(k_{02}\beta-2\xi_{c4}\beta^2), \\ &\qquad [k_{03}m_1-\xi_{c0}-2\xi_{c4}-\xi_{c1}(\varepsilon_2+\varepsilon_7+5\varepsilon_8\|\eta\|)]\big\}. \end{aligned} \tag{124}$$

provided

$$k_{03} > \tfrac{1}{m_1}\left[\xi_{c0}+2\xi_{c4}+\xi_{c1}(\varepsilon_2+\varepsilon_7)+5\xi_{c1}\varepsilon_8\|\eta\|\right], \tag{125}$$

and the conditions for gains in (90) and (91) are met. A sufficient condition for (123) is found from (116) using

$$\|\eta\|^2 \geq \tfrac{2}{\lambda_4}V \text{ and } \|\eta\| \leq \sqrt{\tfrac{2}{\lambda_3}V} \tag{126}$$

to write

$$\dot{V} \leq -2\frac{\lambda_5}{\lambda_4}V + \frac{\varepsilon_0^2}{2\lambda_2}, \tag{127}$$

provided

$$k_{03} > \frac{1}{m_1}\left[\xi_{c0} + 2\xi_{c4} + \xi_{c1}(\varepsilon_2 + \varepsilon_7) + 5\xi_{c1}\varepsilon_8\sqrt{\frac{2}{\lambda_3}V(t)}\right], \tag{128}$$

which yields a new sufficient condition for (123). Solving the differential inequality in (127) yields

$$V \leq V(0)\exp(-\frac{2\lambda_5}{\lambda_4}t) + \frac{\lambda_4\varepsilon_0^2}{4\lambda_2\lambda_5}\left(1 - \exp(-\frac{2\lambda_5}{\lambda_4}t)\right). \tag{129}$$

Then we can write

$$V \leq V(0) + \frac{\lambda_4\varepsilon_0^2}{4\lambda_2\lambda_5}, \tag{130}$$

and from (116) we can write

$$V(0) \leq \frac{\lambda_4}{2}\left\|\eta(0)\right\|^2,$$

and combining these yields

$$V \leq \frac{\lambda_4}{2}\left\|\eta(0)\right\|^2 + \frac{\lambda_4\varepsilon_0^2}{4\lambda_2\lambda_5}, \tag{131}$$

which can be combined with (128) to produce the sufficient condition for given in Theorem 1 to satisfy (123). Substituting (129) into (126) yields

$$\|\eta\| \leq \sqrt{\frac{\lambda_4}{\lambda_3}\left\|\eta(0)\right\|^2\exp(-\frac{2\lambda_5}{\lambda_4}t) + \frac{\lambda_4\varepsilon_0^2}{\lambda_2\lambda_3\lambda_5}(1 - \exp(-\frac{2\lambda_5}{\lambda_4}t))}. \tag{132}$$

Therefore, the result of Theorem 1 can be obtained.

5 Simulation

The output feedback tracking control was simulated using a small quad-rotor unmanned aerial vehicle [13] as depicted in Figure 1. The inertial parameter of the simulation vehicle are borrowed from [14]

$$m = 0.9\ [kg], J = \begin{bmatrix} 0.32 & 0 & 0 \\ 0 & 0.42 & 0 \\ 0 & 0 & 0.63 \end{bmatrix} [kg \cdot m^2]$$

where $g = 9.81[m/\sec^2]$ is acceleration of gravity, and are assumed to be constant while following the trajectory. The desired position and yaw trajectory are given in the following form, respectively

$$p_d(t) = \begin{bmatrix} p_{dx} \\ p_{dy} \\ p_{dz} \end{bmatrix} = \begin{bmatrix} A_x\sin(wt)(1 - e^{(-B_x t^3)}) \\ A_y\cos(wt)(1 - e^{(-B_y t^3)}) \\ A_z(1 - e^{(-B_z t^3)}) \end{bmatrix} \text{(m)}, \tag{133}$$

$$[\psi_d] = \begin{bmatrix} c_o sin(2\frac{\pi}{T}t) \end{bmatrix} \text{(rad)} \tag{134}$$

where $A_x = A_y = 1$, $A_z = 1$, $B_x = B_y = B_z = 5, T = 2.5$, $w = 2 \cdot 2\frac{\pi}{T}$,and $c_o = 1$. The initial position and angle of the quad-rotor at the center of mass are selected as follows

$$p(0) = [0.1, 0.1, 0.1]^T,\ \Theta(0) = [0.1, -0.1, 0.1]^T,\ \hat{x}(0) = [0, 0, -0.1, 0, 0, 0]^T$$

where all parameter estimates $\hat{x}(t)$ are initialized to zero except the position of z-direction ($\hat{p}_z(0) = -0.1$). The initial orientation and constant vector are chosen as follows

$$q(0) = [1, 0, 0, 0]^T, \delta = [0, 0, \delta_3]^T,\ \delta_3 = -1.$$

The constant control parameters for observer and controller were iteratively chosen to be

$$\begin{aligned} k_{01} &= 4,\ k_{02} = 4,\ k_{03} = 2,\ \beta = 2,\ \overline{k}_{03} = 4, \\ k_{r1} &= 5,\ k_{r2} = 1,\ k_z = 45,\ \alpha = 50, \end{aligned}$$

which satisfies the condition of (92).

Figure 3 shows the position tracking of the quad-rotor to the desired trajectory $p_d(t)$. The actual quad-rotor trajectory represented by the solid line follows the desired trajectory represented by the dotted line which is commanded to go up 1[m] high and rotate around circular orbit of radius of 1[m] in the plane. Figure 4 shows position tracking at each axis corresponding to the motion in Figure 3 and the last one shows yaw tracking result to the desired trajectory $\psi_d(t)$. Figure 5 represents the position errors about the each coordinates (x, y, z) and yaw angle errors. Figure 6 shows the control inputs. The translational force input $u_1(t)$ is collectively steady when the UAV rotates at the orbital trajectory. The torque commands $u_2(t)$ periodically changed when they rotate around the circle. Figure 8 shows the estimated output of velocity observer.

6 Conclusion

The goal of designing and output feedback(OFB) controller for a quad-rotor UAV system has been demonstrated mathematically and via a computer simulation. The mathematical result shows that a semi-global uniformly ultimate bounded (SGUUB) tracking result is achieved. The nonlinearities of the damping term were included in the system modeling and it was linearly parameterized because the velocities or other factors are assumed to be unmeasurable. While the output feedback control design was predicated on a hypothetical sensing system that only produces angular and linear positions, it does appear that low-cost GPS or a camera based units may provide justification of this approach. It worth noting that the output feedback design has its advantage over the full state feedback where a full-state feedback controller could be considered a less complicated subset of the current work. We believe this to be the first paper to present such a comprehensive result for quad-rotor tracking control based on only position measurements. Although the focus of this work is the quad-rotor class of aircraft, the results are directly applicable to other aerial vehicles such as the co-axial helicopter and to unmanned underwater vehicles.

Acknowledgement This work is supported in part by a DOC Grant, an ARO Automotive Center Grant, a DOE Contract, a Honda Corporation Grant and a DARPA Contract.

References

[1] A. Mokhtari and A. Benallegue, "Dynamic Feedback Controller of Euler Angles and Wind Parameters Estimation for a quad-rotor Unmanned Aerial Vehicle", *Proc. 2004 IEEE International Conference on Robotics and Automation*, Vol 3, May 2004, pp. 2359 - 2366.

[2] J. S. Jangy and C. J. Tomlin, "Longitudinal Stability Augmentation System "Design for the DragonFly UAV Using a Single GPS Receiver", *Proc. AIAA Guidance, Navigation, and Control Conference and Exhibit,* Austin, Texas, August 2003.

[3] T. Hamel, R. Mahony, R. Lozano, and J. Ostrowski, "Dynamic Modelling and Configuration Stabilization for An X4-Flyer", *Proc. IFAC World Congress*, Barcelona, Spain, 2002.

[4] P. Castillo, A. Dzul, and R. Lozano, "Real-time Stabilization and Tracking of a Four-rotor Mini Rotorcraft", *IEEE Transactions on Control Systems Technology*, Volume 12, Issue 4, July 2004, pp. 510 - 516.

[5] A. Tayebi and S. McGilvray, "Attitude stabilization of a four-rotor aerial robot", *Proc. 43rd IEEE Conference on Decision and Control,* Vol. 2, Dec. 2004, pp. 1216 - 1221.

[6] V. Chitrakaran, D. M. Dawson, J. Chen, and M. Feemster, "Vision Assisted Autonomous Landing of an Unmanned Aerial Vehicle", *Proc. 44th IEEE Conference on Decision and Control*, Seville, Spain, Dec. 2005, pp. 1465-1470.

[7] D. Suter, T. Hamel, and R. Mahony, "Visual Servo Control Using Homography Estimation for the Stabilization of an X4-Flyer", *Proc. 41st IEEE Conference on Decision and Control*, Las Vegas, NV, 2002, pp. 2872-2877.

[8] O. Shakernia, Y. Ma, T. J. Koo, and S. Sastry, "Landing an Unmanned Air Vehicle: Vision Based Motion Estimation and Nonlinear Control", *Asian Journal of Control*, Vol. 1, No. 3, pp. 128-145, 1999.

[9] M. Queiroz, D. Dawson, S. Nagarkatti, and F. Zang, *Lyapunov-based Control of Mechanical Systems*, Birkhauser, 2000.

[10] H. Berghuis and H. Nijmeijer, "A Passivity Approach to Controller-Observer Design for Robots", *IEEE Transaction Robotics and Automation*, Vol 9, No 6, Dec 1993, pp. 740 - 754.

[11] W. E. Dixon, A. Bethal, and D. M. Dawson, S. P. Nagarkatti, *Nonlinear control of Engineering Systems: A Lyapunov-based Approach*, Birkhauser, 2003.

[12] T.I. Fossen, *Marine Control Systems : Guidance, Navigation, and Control of Ships, Rigs and Undewater Vehicles*, Marine Cybernetics, 2002.

[13] Dragonfly x-pro : http://www.rctoys.com/draganflyerxpro.php

[14] E.T. King, " "Distributed Coordination and Control Experiments on a Multi-UAV Testbed", Master Thesis in Aeronautics and Astronautics, MIT, Sep. 2004.

[15] M. Buschmann, J. Bange and P. Vörsmann, "A Miniature Unmanned Aerial Vehicle (Mini-UAV) for Meteorological Purposes", *Proc. 16th Symposium on Boundary Layers and Turbulence*, Aug. 2004.

[16] DongBin Lee, Timothy Burg, Bin Xian, and Darren Dawson, "Output Feedback Tracking Control of an Underactuated Quad-Rotor UAV", CRB Technical Report, CU/CRB/, http://www.ece.clemson.edu/crb/publictn/tr.htm, 2006.

A Development of Dynamic Model in the Inertial frame

The dynamic equation of (1) describing the dynamics of the quad-rotor can be directly written in the form

$$\bar{M}\dot{\Phi}(\dot{v},\dot{\omega}) = \bar{C}(R,T)D(R,T)\dot{x} + \bar{h}(R,T,\dot{x}) + \bar{G}(R) + \bar{B}\bar{U} \tag{135}$$

using the definition of $\Phi(v,\omega)$ in (10) and the following substitutions

$$\begin{aligned}
\bar{M} &= \begin{bmatrix} mI_3 & O_{3x3} \\ O_{3x3} & J \end{bmatrix} \in \Re^{6x6},\ \bar{C}(R,T) = \begin{bmatrix} -mS(\omega) & O_{3x3} \\ O_{3x3} & S(J\omega) \end{bmatrix} \in \Re^{6x6}, \\
\bar{G}(R) &= \begin{bmatrix} G(R) \\ O_{3x1} \end{bmatrix} \in \Re^{6},\ \bar{h}(R,T,\dot{x}) = \begin{bmatrix} N_1(v) \\ N_2(\omega) \end{bmatrix} \in \Re^{6}, \\
\bar{B} &= \begin{bmatrix} B_1 & O_{3x3} \\ O_{3x1} & B_2 \end{bmatrix} \in \Re^{6x4},\ \bar{U} = \begin{bmatrix} u_1 \\ u_2 \end{bmatrix} \in \Re^{4}\ .
\end{aligned} \tag{136}$$

The time derivative of $\Phi(v,\omega)$ in (10) can be related to $\ddot{x}(t)$ by differentiating (9) and applying the definition

$$\frac{d}{dt}\left(D(R,T)\right) \triangleq \bar{D}(R,T,\dot{x}) \tag{137}$$

where

$$\begin{aligned}
\frac{d}{dt}\left(D(R,T)\right) &= \begin{bmatrix} \frac{d}{dt}(R^T) & O_{3x3} \\ O_{3x3} & \frac{d}{dt}(T^{-1}(\Theta)) \end{bmatrix} \in \Re^{6x6},\ \frac{d}{dt}(R^T) = \dot{R}^T = -S(\omega)R^T \text{ and} \\
\frac{d}{dt}(T^{-1}(\Theta)) &= \frac{\partial}{\partial\Theta}(T^{-1}(\Theta))\dot{\Theta} \in \Re^{3x3} \text{ where } \frac{\partial}{\partial\Theta}(T^{-1}(\Theta)) \in \Re^{3x3x3} \text{ is a tensor,}
\end{aligned} \tag{138}$$

to yield

$$\dot{\Phi}(\dot{v},\dot{\omega}) = \frac{d}{dt}\left(D(R,T)\right)\dot{x} + D(R,T)\ddot{x} = \bar{D}(R,T,\dot{x})\dot{x} + D(R,T)\ddot{x}. \tag{139}$$

Multiplying by $\bar{M}(\cdot)$, substituting from (135) for $\bar{M}\dot{\Phi}(\dot{v},\dot{\omega})$ and from (9) for $\Phi(v,\omega)$, and arranging terms yields

$$\bar{M}D(R,T)\ddot{x} = \bar{C}(R,T)D(R,T)\dot{x} - \bar{M}\bar{D}(R,T,\dot{x})\dot{x} + \bar{h}(R,T,\dot{x}) + \bar{G}(R) + \bar{B}\bar{U}. \tag{140}$$

It can be shown that $D^T(R,T) = \left[R(q), O_{3x3}; O_{3x3}, T^{-T}\right] \in \Re^{6x6}$. After multiplying (140) by $D^T = D^T(R,T)$, we have

$$D^T\bar{M}D(R,T)\ddot{x} = D^T\left(\bar{C}(R,T)D(R,T) - \bar{M}\bar{D}(R,T,\dot{x})\right)\dot{x} + D^T\bar{h}(R,T,\dot{x}) + D^T\bar{G}(R) + D^T\bar{B}\bar{U}. \tag{141}$$

Equation (141) is now written in the compact form

$$M^*(R,T)\ddot{x} = N^*(R,T,\dot{x})\dot{x} + h^*(R,T,\dot{x}) + G^*(R) + B^*(R,T)\bar{U} \tag{142}$$

where the corresponding matrices were substituted as follows

$$\begin{aligned}
M^*(R,T) &\triangleq D^T(R,T)\bar{M}D(R,T) = [mI_3, O_{3x3}; O_{3x3}, T^{-T}(\Theta)JT^{-1}(\Theta)], \\
N^*(R,T,\dot{x}) &\triangleq D^T(R,T)\left(\bar{C}(R,T)D(R,T) - \bar{M}\bar{D}(R,T,\dot{x})\right) \text{ in (209)} \\
h^*(R,T,\dot{x}) &\triangleq D^T(R,T)\bar{h}(R,T,\dot{x}) = [RN_1(v); T^{-T}(\Theta)N_2(\omega)], \\
G^*(R) &\triangleq D^T(R,T)\bar{G}(R) = [RG(R); O_{3x1}], \\
B^*(R,T) &\triangleq D^T(R,T)\bar{B} = [RB_1, O_{3x3}; O_{3x1}, T^{-T}(\Theta)B_2].
\end{aligned} \tag{143}$$

B Proof of Model Property P1

The validity of the skewed symmetric relationship in P1 is shown below. The definitions of $M^*(R,T)$ and $N^*(R,T,\dot{x})$ from (143) in Appendix A are first applied to the matrix term of P1, that is

$$\xi^T \left(\frac{d}{dt} \left(M^*(R,T) \right) + 2N^*(R,T,\dot{x}) \right) \xi = 0, \ \forall \ \xi \in \Re^6$$

to yield

$$\begin{aligned} \xi^T \left(\tfrac{d}{dt} \left(M^*(R,T) \right) + 2N^*(R,T,\dot{x}) \right) \xi &= \xi^T \left(\tfrac{d}{dt} \left(D^T(R,T) \bar{M} D(R,T) \right) \right) \xi \\ &\quad + \xi^T \left(2D^T(R,T) \left(\bar{C}(R,T) D(R,T) - \bar{M} \bar{D}(R,T,\dot{x}) \right) \right) \xi. \end{aligned} \tag{144}$$

The definition of $\bar{D}(R,T,\dot{x})$ from (137) in Appendix A is now applied and terms collected to yield

$$\begin{aligned} \xi^T \left(\frac{d}{dt} \left(M^*(R,T) \right) + 2N^*(R,T,\dot{x}) \right) \xi &= \xi^T \left(2D^T(R,T) \bar{C}(R,T) D(R,T) \right) \xi \\ &\quad + \xi^T \left(\bar{D}^T(R,T,\dot{x}) \bar{M} D(R,T) - D^T \bar{M} \bar{D}(R,T,\dot{x}) \right) \xi \end{aligned} \tag{145}$$

where $\bar{M}(\cdot)$ is a constant matrix and hence $\frac{d}{dt}\bar{M} = 0$ has been used. It is now useful to invoke the symmetric property of $\bar{M}(\cdot)$ to write

$$\xi^T \left(\bar{D}^T(R,T,\dot{x}) \bar{M} D(R,T) \right) \xi - \xi^T \left(D^T \bar{M} \bar{D}(R,T,\dot{x}) \right) \xi = 0, \tag{146}$$

which allows (145) to be written as

$$\xi^T \left(\frac{d}{dt} \left(M^*(R,T) \right) + 2N^*(R,T,\dot{x}) \right) \xi = 2\xi^T D^T(R,T) \bar{C}(R,T) D(R,T) \xi. \tag{147}$$

It is now possible to introduce a new vector $\xi' \in \Re^6$ defined as $\xi' = D(R,T)\xi$ in order to rewrite (147) as

$$\xi^T \left(\frac{d}{dt} \left(M^*(R,T) \right) + 2N^*(R,T,\dot{x}) \right) \xi = 2\xi'^T \bar{C}(R,T) \xi' \tag{148}$$

where it is clear that if $\bar{C}(R,T)$ is skew symmetric then the right-hand side of (148) is zero. The definition of $\bar{C}(R,T)$ in (136) is substituted, and ξ' partitioned into subvectors to write (148) as

$$\xi'^T \bar{C}(R,T) \xi' = \begin{bmatrix} \xi_1'^T & \xi_2'^T \end{bmatrix} \begin{bmatrix} -mS(\omega) & O_{3\text{x}3} \\ O_{3\text{x}3} & S(J\omega) \end{bmatrix} \begin{bmatrix} \xi_1' \\ \xi_2' \end{bmatrix} = -m\xi_1'^T S(\omega) \xi_1' + \xi_2'^T S(J\omega) \xi_2' \tag{149}$$

where it is clear that the skew symmetry property of $S(\omega)$ and $S(J\omega)$ can be invoked to write

$$2\xi'^T \bar{C}(R,T) \xi' = 0, \tag{150}$$

and hence,

$$\xi^T \left(\frac{d}{dt} \left(M^*(R,T) \right) + 2N^*(R,T,\dot{x}) \right) \xi = 0. \tag{151}$$

C Development and Derivative of Control Signal $\bar{u}_1(t)$

The term of interest is first repeated from (30) and the definition of $\dot{r}\ (t)$ in (27) is inserted as a reminder to form

$$\dot{r}= \left[\begin{array}{c} -S(\omega)r_p + \frac{\alpha}{m}e_v - R^T\ \ddot{p}_d + \alpha(\frac{1}{m}-1)R^T\dot{p}_d + G(R) \\ -\omega_{zd} \end{array} \right] + \left[\begin{array}{c} N_1(v) \\ 0 \end{array} \right] + \left[\begin{array}{c} -S(\delta)\omega + B_1 u_1 \\ T_z(\Theta)\omega \end{array} \right]. \tag{152}$$

With $B_1 = [0, 0, 1]^T$, it can be seen that the control input $u_1(t)$ will only act on the z-axis translational dynamics. A new control signal will be injected that creates control signals to all three translational axes; these injected control signals then become the tracking objectives for the rotational dynamics. The control term from (152) can be divided into two parts; $B_\mu(\cdot)$ defined in (34) and $\mu(t) \in \Re^4$, and hence, becomes as follows

$$\left[\begin{array}{c} -S(\delta)\omega + B_1 u_1 \\ T_z(\Theta)\omega \end{array} \right] = \left[\begin{array}{cc} -S(\delta) & B_1 \\ T_z(\Theta) & 0 \end{array} \right] \left[\begin{array}{c} \omega \\ u_1 \end{array} \right] = B_\mu \mu. \tag{153}$$

The term $\bar{u}_1(t) = [\bar{\bar{u}}_1^T, u_1] \in \Re^4$ with $\bar{\bar{u}}_1\ (t) \in \Re^3$ can be added and subtracted to $\mu(t)$ of (153) as follows

$$\mu = +\bar{u}_1 - \bar{u}_1 + \left[\begin{array}{c} \omega \\ u_1 \end{array} \right] = \bar{u}_1 + \left[\begin{array}{c} \omega \\ u_1 \end{array} \right] - \left[\begin{array}{c} \bar{\bar{u}}_1 \\ u_1 \end{array} \right] = \bar{u}_1 + \left[\begin{array}{c} \omega - \bar{\bar{u}}_1 \\ 0 \end{array} \right]. \tag{154}$$

The term $z(t)$ can be defined to be a measure of the closeness of $\omega(t)$ to $\bar{\bar{u}}_1\ (t)$ as

$$z = \omega - \bar{\bar{u}}_1,$$

which can then be written as

$$z = \omega - B_z \bar{u}_1 \text{ where } B_z = \left[\begin{array}{cccc} 1 & 0 & 0 & 0 \\ 0 & 1 & 0 & 0 \\ 0 & 0 & 1 & 0 \end{array} \right]. \tag{155}$$

It is interesting to note that if $z(t)$ is zero then the control signal $\bar{u}_1(t)$ has been effectively injected into the open-loop filtered tracking error dynamics. The manipulation of $\mu(t)$ can be continued from (154) using the definition of $z(t)$ to yield

$$\mu = \bar{u}_1 + \left[\begin{array}{c} z \\ 0 \end{array} \right]. \tag{156}$$

After multiplying $\mu(t)$ of (156) by $B_\mu(\cdot)$ of (153), we have

$$B_\mu \mu = B_\mu \bar{u}_1 + B_\mu \left[\begin{array}{c} z \\ 0 \end{array} \right], \tag{157}$$

and thus

$$\left[\begin{array}{c} -S(\delta)\omega + B_1 u_1 \\ T_z(\Theta)\omega \end{array} \right] = B_\mu \bar{u}_1 + B_\mu \left[\begin{array}{c} z \\ 0 \end{array} \right]. \tag{158}$$

The derivative of $\dot{\bar{u}}_1\ (t)$ is obtained by taking time derivative of (66). It is perhaps more illustrative to abbreviate (66) as

$$\bar{u}_1 = B_\mu^{-1} U \tag{159}$$

where $B_\mu^{-1}(\cdot)$ is

$$B_\mu^{-1} = \begin{bmatrix} 0 & -\frac{1}{\delta_3} & 0 & 0 \\ \frac{1}{\delta_3} & 0 & 0 & 0 \\ -\frac{1}{\delta_3}\frac{\mathrm{s}\phi}{\mathrm{c}\phi} & 0 & 0 & \frac{\mathrm{c}\theta}{\mathrm{c}\phi} \\ 0 & 0 & 1 & 0 \end{bmatrix}, \tag{160}$$

and hence, after differentiation, we have

$$\dot{\bar{u}}_1 \triangleq \frac{d}{dt}(B_\mu^{-1})U + (B_\mu^{-1})\frac{d}{dt}U \tag{161}$$

where is now clear that two derivatives are required. Term by term differentiation of $B_\mu^{-1}(\cdot)$ yields

$$\frac{d}{dt}(B_\mu^{-1}) = \begin{bmatrix} 0 & 0 & 0 & 0 \\ 0 & 0 & 0 & 0 \\ -\frac{1}{\delta_3}\frac{\dot{\hat{\phi}}}{\mathrm{c}^2\phi} & 0 & 0 & \frac{\text{-c}\phi\mathrm{s}\theta\cdot\dot{\hat{\theta}}+\mathrm{s}\phi\mathrm{c}\theta\dot{\hat{\phi}}}{\mathrm{c}^2\phi} \\ 0 & 0 & 0 & 0 \end{bmatrix} \tag{162}$$

where $\Theta(t)$ is measurable and $\dot{\hat{\phi}}\,(t) = T_x(\Theta)\hat{\omega}$ and $\dot{\hat{\theta}}\,(t) = T_y(\Theta)\hat{\omega}$ are estimated from (35). Next, the time derivative of $U(t)$ is rewritten from (80) as follows

$$\begin{aligned} \frac{d}{dt}U &= -k_r\,\dot{\hat{r}} + \begin{bmatrix} -\dfrac{d}{dt}\left(Y_1(\hat{v})\theta_1\right) - \frac{\alpha}{m}\,\dot{\hat{e}}_v - \frac{1}{m}\,\dot{\hat{e}}_p \\ 0 \end{bmatrix} \\ &\quad + \begin{bmatrix} S(\hat{\omega})\left(\frac{\alpha}{m}R^T\dot{p}_d - \alpha R^T\dot{p}_d - R^T\,\ddot{p}_d + mgR^TE_z\right) + \alpha\left(1-\frac{1}{m}\right)R^T\,\ddot{p}_d + R^T\,\dddot{p}_d \\ \dot{\omega}_{zd} \end{bmatrix} \end{aligned}$$

where (56), (57), and (63) are utilized. The term $Y_1(\hat{v})\theta_1$ is a general representation of the nonlinear aerodynamic damping, and therefore, the time derivative cannot be written explicitly until a specific model has been assumed (such a model is assumed for use in the Simulation section and the resulting derivative $\frac{d}{dt}\left(Y_1(\hat{v})\theta_1\right)$ is calculated in Appendix $E.3$. Therefore, $\dot{\bar{u}}_1\,(t)$ is obtained by substituting (162) and (80) into (79).

D Details of Stability Analysis

Development of an upper bound $\left\|\dot{\hat{x}}\right\|$ in (118) requires bounds for $\dot{\hat{p}}\,(t)$ and $\dot{\hat{\Theta}}\,(t)$.

D.1 Upper Bound for $\dot{\hat{p}}\,(t)$

As a starting point for the bound on $\dot{\hat{p}}\,(t)$, $e_v(t)$ in (19) is substituted into the definition of $r_p(t)$ in (25) and the result solved for $v(t)$ to yield

$$v = \frac{1}{m}(r_p - \alpha e_p - \delta + R^T\dot{p}_d). \tag{163}$$

We can now use (163) and $\tilde{v}(t) = v - \hat{v}$ to obtain

$$\hat{v} = -\tilde{v} + \frac{1}{m}\left(r_p - \alpha e_p - \delta + R^T\dot{p}_d\right). \tag{164}$$

Now $\dot{\hat{p}}\,(t)$ can be expressed by using (35) and substituting from (164), as follows

$$\begin{aligned}\dot{\hat{p}} &= R\hat{v} \\ &= -R\tilde{v} + \frac{1}{m}R\left(r_p - \alpha e_p - \delta + R^T\dot{p}_d\right), \end{aligned} \tag{165}$$

and then we utilize (35), (165), and $\dot{\tilde{p}}\,(t) = R\tilde{v}$ to yield

$$\dot{\hat{p}} = -\dot{\tilde{p}} + \frac{1}{m}R\left(r_p - \alpha e_p - \delta + R^T\dot{p}_d\right). \tag{166}$$

The triangle inequality can be utilized to create an upper bound for $\dot{\hat{p}}\,(t)$ in (166) as follows

$$\|\dot{\hat{p}}\| \leq \left\|\dot{\tilde{p}}\right\| + \left\|\frac{R}{m}\right\| \|r_p\| + \alpha\left\|\frac{R}{m}\right\| \|e_p\| + \left\|\frac{R}{m}\right\| \left\|\delta + R^T\dot{p}_d\right\|, \tag{167}$$

which can be further bounded as

$$\|\dot{\hat{p}}\| \leq \left\|\dot{\tilde{p}}\right\| + \varepsilon_1\|r_p\| + \alpha\varepsilon_1\|e_p\| + \varepsilon_2 \tag{168}$$

where

$$\varepsilon_1 \triangleq \frac{1}{m}\sup_{\forall\theta}\|R\|_{i\infty}, \;\; \varepsilon_2 \triangleq \frac{1}{m}\sup_{\forall\theta}\|R\|_{i\infty}\left(\|\delta\| + \sup_{\forall\theta}\left\|R^T\right\|_{i\infty}\sup_{\forall t}\|\dot{p}_d\|\right). \tag{169}$$

D.2 Upper Bound for $\dot{\hat{\Theta}}\,(t)$

To begin the development of a bound for $\dot{\hat{\Theta}}\,(t)$, $\tilde{\omega}(t) = \omega - \hat{\omega}$ is solved for $\hat{\omega}(t)$ producing

$$\hat{\omega} = \omega - \tilde{\omega}. \tag{170}$$

After multiplying (170) by the transformation matrix $T(\Theta)$, we have

$$T(\Theta)\hat{\omega} = T(\Theta)\omega - T(\Theta)\tilde{\omega}, \tag{171}$$

which is equivalent to

$$\dot{\hat{\Theta}} = T(\Theta)\omega - \dot{\tilde{\Theta}}. \tag{172}$$

The definition of $z(t)$ in (31) is solved for $\omega(t)$ to yield

$$\omega = z + B_z\bar{u}_1, \tag{173}$$

and the control $\bar{u}_1(t)$ in (66) is substituted into (173) to yield

$$\begin{aligned}\omega &= z + B_z B_\mu^{-1}\left(-k_r r + k_r\begin{bmatrix} m\tilde{v} \\ 0 \end{bmatrix}\right. \\ &\quad \left. + \begin{bmatrix} -\frac{\alpha}{m}(r_p - \alpha e_p - \delta) + \alpha\tilde{v} - \frac{e_p}{m} - \alpha(\frac{1}{m} - 1)R^T\dot{p}_d + R^T\ddot{p}_d - G(R) - Y_1(\hat{v})\theta_1 \\ \omega_{zd} \end{bmatrix}\right) \end{aligned} \tag{174}$$

where $\tilde{r}_p(t) = m\tilde{v}$ was used for $\tilde{r}(t)$, $e_v(t)$ was substituted from (25), and $\tilde{r}_p(t)$ was substituted from (69). By substituting (174) into (172), $\dot{\hat{\Theta}}(t)$ can be expressed as follows

$$\begin{aligned}\dot{\hat{\Theta}} &= -\dot{\tilde{\Theta}} + Tz + TB_zB_\mu^{-1}\left(-k_r r + k_r \begin{bmatrix} m\tilde{v} \\ 0 \end{bmatrix}\right. \\ &\left. + \begin{bmatrix} -\frac{\alpha}{m}(r_p - \alpha e_p - \delta) + \alpha\tilde{v} - \frac{e_p}{m} - \alpha(\frac{1}{m}-1)R^T\dot{p}_d + R^T\ddot{p}_d - G(R) - Y_1(\hat{v})\theta_1 \\ \omega_{zd} \end{bmatrix}\right). \quad (175)\end{aligned}$$

In order to combine the two $\tilde{v}(t)$ terms, the matrix $B_z^T(\cdot)$,

$$B_z^T = \begin{bmatrix} I_3 \\ O_{1x3} \end{bmatrix} \in \Re^{4x3}, \quad (176)$$

and the equality $R^T\dot{\tilde{p}}(t) = \tilde{v}(t)$ from (35) are used to formulate the equality

$$\begin{bmatrix} \tilde{v} \\ 0 \end{bmatrix} = B_z^T\tilde{v} = B_z^TR^T\dot{\tilde{p}}, \quad (177)$$

which is then substituted into (175) to yield

$$\begin{aligned}\dot{\hat{\Theta}} &= -\dot{\tilde{\Theta}} + Tz + TB_zB_\mu^{-1}B_z^T(k_rm + \alpha)R^T\dot{\tilde{p}} - TB_zB_\mu^{-1}k_rr \\ &+ TB_zB_\mu^{-1}\begin{bmatrix} -\frac{\alpha}{m}r_p - Y_1(\hat{v})\theta_1 + \frac{e_p}{m}(\alpha^2-1) + \frac{\alpha}{m}\delta - \alpha(\frac{1}{m}-1)R^T\dot{p}_d + R^T\ddot{p}_d - G(R) \\ \omega_{zd} \end{bmatrix}. \quad (178)\end{aligned}$$

From the A2, the nonlinear aerodynamic damping term $Y_1(\hat{v})\theta_1$ in (178) can be bounded by the following expression

$$\|Y_1(\hat{v})\theta_1\| \leq \xi_{c4}\|\hat{v}\|. \quad (179)$$

It can be used to show $\tilde{v}(t) = R^T\dot{\tilde{p}}$ which can be substituted into (164) to show that

$$\hat{v} = -R^T\dot{\tilde{p}} + \frac{1}{m}r_p - \frac{\alpha}{m}e_p - \frac{1}{m}(\delta - R^T\dot{p}_d). \quad (180)$$

$\hat{v}(t)$ can now be upper bounded in the same manner as $\|\dot{\hat{p}}\|$ in (167) as follows

$$\|\hat{v}\| \leq \left\|R^T\right\|\left\|\dot{\tilde{p}}\right\| + \frac{1}{m}\|r_p\| + \frac{\alpha}{m}\|e_p\| + \frac{1}{m}\left\|\delta + R^T\dot{p}_d\right\|. \quad (181)$$

The definition of $r(t)$ in (26) leads to the bound on $r_p(t)$ given by

$$\|r_p\| \leq \|r\|. \quad (182)$$

The bound in (179) can now be upper bounded in the manner

$$\|Y_1(\hat{v})\theta_1\| \leq \xi_{c4}\left[\left\|R^T\right\|\left\|\dot{\tilde{p}}\right\| + \frac{1}{m}\|r_p\| + \frac{\alpha}{m}\|e_p\| + \frac{1}{m}\left\|\delta + R^T\dot{p}_d\right\|\right], \quad (183)$$

by using (181). An upper bound can now be developed for $\dot{\hat{\Theta}}(t)$ from (178) as follows

$$\begin{aligned}
\left\|\dot{\hat{\Theta}}\right\| &\leq \left\|\dot{\tilde{\Theta}}\right\| + \|T\| \cdot \|z\| + \left[\left\|TB_z B_\mu^{-1} B_z^T (k_r m + \alpha) R^T\right\| + \left\|TB_z B_\mu^{-1} B_z^T\right\| \cdot \xi_{c4} \left\|R^T\right\|\right] \left\|\dot{\tilde{p}}\right\| \\
&+ \left[\left\|TB_z B_\mu^{-1} B_z^T (\frac{\alpha}{m} + k_r)\right\| + \left\|TB_z B_\mu^{-1} B_z^T\right\| \frac{\xi_{c4}}{m}\right] \|r\| \\
&+ \left[\left\|TB_z B_\mu^{-1} B_z^T (\frac{\alpha^2}{m} - \frac{1}{m})\right\| + \frac{\alpha}{m} \xi_{c4} \left\|TB_z B_\mu^{-1} B_z^T\right\|\right] \|e_p\| \\
&+ \left\|TB_z B_\mu^{-1} B_z^T\right\| \cdot \left\|\frac{\alpha}{m}\delta + \alpha(\frac{1}{m} - 1) R^T \dot{p}_d + R^T \ddot{p}_d + G(R)\right\| \\
&+ \left\|TB_z B_\mu^{-1} B_3\right\| \cdot \|\omega_{zd}\| + \left\|TB_z B_\mu^{-1} B_z^T\right\| \cdot \frac{\xi_{c4}}{m} \left\|\delta + R^T \dot{p}_d\right\|
\end{aligned} \tag{184}$$

where the abbreviation $T = T(\Theta)$ and $B_3 = [0, 0, 0, 1]^T$ for matrix dimension were used, and (182), (183) have been utilized. The following constants are introduced to simplify expression (184)

$$\begin{aligned}
\varepsilon_3 &= \varepsilon_4 \varepsilon_9 \left\|B_z B_\mu^{-1} B_z^T (k_r m + \alpha)\right\|_{i\infty} + \varepsilon_4 \varepsilon_9 \left\|B_z B_\mu^{-1} B_z^T\right\|_{i\infty} \xi_{c4} \\
\varepsilon_4 &= \sup_{\forall \theta} \|T\|_{i\infty}, \\
\varepsilon_5 &= \varepsilon_4 \left\|B_z B_\mu^{-1} B_z^T (\frac{\alpha}{m} + k_r)\right\|_{i\infty} + \frac{\xi_{c4}}{m} \varepsilon_4 \left\|B_z B_\mu^{-1} B_z^T\right\|_{i\infty} \\
\varepsilon_6 &= \varepsilon_4 \left\|B_z B_\mu^{-1} B_z^T (\frac{\alpha^2}{m} - \frac{1}{m})\right\|_{i\infty} + \frac{\alpha}{m} \xi_{c4} \varepsilon_4 \left\|B_z B_\mu^{-1} B_z^T\right\|_{i\infty} \\
\varepsilon_7 &= \varepsilon_4 \left\|B_z B_\mu^{-1} B_z^T\right\|_{i\infty} \left(\frac{\alpha}{m} \|\delta\| + \alpha \left|\frac{1}{m} - 1\right| \varepsilon_9 \sup_{\forall t} \|\dot{p}_d\| + \varepsilon_9 \sup_{\forall t} \left\|\ddot{p}_d\right\| + \|G(R)\|\right) \\
&\quad + \varepsilon_4 \left\|B_z B_\mu^{-1} B_3\right\|_{i\infty} \sup_{\forall t} \|\omega_{zd}\| + \frac{\xi_{c4}}{m} \varepsilon_4 \left\|B_z B_\mu^{-1} B_z^T\right\|_{i\infty} \left(\|\delta\| + \varepsilon_9 \sup_{\forall t} \|\dot{p}_d\|\right) \\
\varepsilon_9 &= \sup_{\forall \theta} \left\|R^T\right\|_{i\infty},
\end{aligned} \tag{185}$$

thereby, creating the final bound for $\dot{\hat{\Theta}}(t)$ as follows

$$\left\|\dot{\hat{\Theta}}\right\| \leq \left\|\dot{\tilde{\Theta}}\right\| + \varepsilon_4 \|z\| + \varepsilon_3 \left\|\dot{\tilde{p}}\right\| + \varepsilon_5 \|r\| + \varepsilon_6 \|e_p\| + \varepsilon_7. \tag{186}$$

The definition of $\dot{\hat{x}}(t)$ is formed from the right-hand terms in (35) and (36) and an upper bound applied as follows

$$\left\|\dot{\hat{x}}\right\| = \left\|\begin{bmatrix} \dot{\hat{p}} \\ \dot{\hat{\Theta}} \end{bmatrix}\right\| \leq \left\|\dot{\hat{p}}\right\| + \left\|\dot{\hat{\Theta}}\right\|. \tag{187}$$

The bound in (168) for $\dot{\hat{p}}(t)$ and the bound in (186) for $\dot{\hat{\Theta}}(t)$ can now be substituted into (187) to create an upper bound for $\dot{\hat{x}}(t)$ in the manner

$$\begin{aligned}
\left\|\dot{\hat{x}}\right\| &\leq \left\|\dot{\tilde{p}}\right\| + \varepsilon_1 \|r_p\| + \alpha \varepsilon_1 \|e_p\| + \varepsilon_2 \\
&\quad + \left\|\dot{\tilde{\Theta}}\right\| + \varepsilon_4 \|z\| + \varepsilon_3 \left\|\dot{\tilde{p}}\right\| + \varepsilon_5 \|r\| + \varepsilon_6 \|e_p\| + \varepsilon_7.
\end{aligned} \tag{188}$$

Additionally, the terms $\dot{\tilde{p}}(t)$ and $\dot{\tilde{\Theta}}(t)$ can be individually bounded as

$$\left\|\dot{\tilde{p}}\right\| \leq \left\|\dot{\tilde{\hat{x}}}\right\|, \quad \left\|\dot{\tilde{\Theta}}\right\| \leq \left\|\dot{\tilde{\hat{x}}}\right\|. \tag{189}$$

Now the substitution of the bounds from (189) and (182) into (188) yields

$$\left\|\dot{\hat{x}}\right\| \leq (2+\varepsilon_3)\left\|\dot{\tilde{\hat{x}}}\right\| + \varepsilon_4 \|z\| + (\varepsilon_1+\varepsilon_5)\|r\| + (\alpha\varepsilon_1+\varepsilon_6)\|e_p\| + \varepsilon_2 + \varepsilon_7. \tag{190}$$

E Simulation Notes

E.1 Desired Trajectory

The desired trajectory along the three linear directions is given as follows. The desired trajectories for the x-axis are

$$\begin{aligned}
p_{dx} &= A_x \sin(wt)(1-e^{(-0.5t^3)}) \\
\dot{p}_{dx} &= A_x(w\cos(wt)(1-e^{(-0.5t^3)}) + \sin(wt)1.5t^2e^{(-0.5t^3)}) \\
\ddot{p}_{dx} &= A_x(-(w)^2\sin(wt)(1-e^{(-0.5t^3)}) + 2w\cos(wt)1.5t^2e^{(-0.5t^3)} \\
&\quad + \sin(wt)3te^{(-0.5t^3)} - \sin(wt)(1.5t^2)^2e^{(-0.5t^3)}) \\
\dddot{p}_{dx} &= A_x(-(w)^3\cos(wt)(1-e^{(-0.5t^3)}) - (w)^2\sin(wt)1.5t^2e^{(-0.5t^3)} \\
&\quad -2((w)^2\sin(wt)1.5t^2e^{(-0.5t^3)} + 3w\cos(wt)te^{(-0.5t^3)} \\
&\quad -w\cos(wt)(1.5t^2)^2e^{(-0.5t^3)}) + (3w\cos(wt)te^{(-0.5t^3)} + \sin(wt)3e^{(-0.5t^3)} \\
&\quad -4.5\sin(wt)t^3e^{(-0.5t^3)}) - w\cos(wt)(1.5t^2)^2e^{(-0.5t^3)} - 2\sin(wt)(1.5t^2) \\
&\quad 3te^{(-0.5t^3)} + \sin(wt)(1.5t^2)^3e^{(-0.5t^3)}),
\end{aligned} \tag{191}$$

for the y-axis are

$$\begin{aligned}
p_{dy} &= A_y \cos(wt)(1-e^{(-0.5t^3)}) \\
\dot{p}_{dy} &= A_y(-w\sin(wt)(1-e^{(-0.5t^3)}) + \cos(wt)1.5t^2e^{(-0.5t^3)}) \\
\ddot{p}_{dy} &= A_y(-(w)^2\cos(wt)(1-e^{(-0.5t^3)}) - 2w\sin(wt)1.5t^2e^{(-0.5t^3)} \\
&\quad + \cos(wt)3te^{(-0.5t^3)} - \cos(wt)(1.5t^2)^2e^{(-0.5t^3)}) \\
\dddot{p}_{dy} &= A_y((w)^3\sin(wt)(1-e^{(-0.5t^3)})) - (w)^2\cos(wt)1.5t^2e^{(-0.5t^3)} \\
&\quad -2((w)^2\cos(wt)1.5t^2e^{(-0.5t^3)} + w\sin(wt)3te^{(-0.5t^3)} \\
&\quad -w\sin(wt)(1.5t^2)^2e^{(-0.5t^3)}) - w\sin(wt)3te^{(-0.5t^3)} + \cos(wt)3e^{(-0.5t^3)} \\
&\quad -\cos(wt)3t(1.5t^2)e^{(-0.5t^3)} + w\sin(wt)(1.5t^2)^2e^{(-0.5t^3)} - \cos(wt)2(1.5t^2) \\
&\quad 3te^{(-0.5t^3)} + \cos(wt)(1.5t^2)^3e^{(-0.5t^3)}),
\end{aligned}$$

and for the z-axis are

$$\begin{aligned}
p_{dz} &= A_z(1-e^{(-0.5t^3)}) \\
\dot{p}_{dz} &= A_z 1.5t^2e^{(-0.5t^3)} \\
\ddot{p}_{dz} &= A_z 1.5(2t-1.5t^4)e^{(-0.5t^3)} \\
\dddot{p}_{dz} &= A_z 1.5((2-6t^3)-(2t-1.5t^4)1.5t^2)e^{(-0.5t^3)}.
\end{aligned}$$

E.2 Nonlinear Aerodynamic Damping Term

The nonlinearities of the aerodynamic damping terms $N_1(v)$, $N_2(w)$ were included in the system modeling (1) and specific knowledge of the system model is given by

$$\begin{aligned} N_1(v) &= \begin{bmatrix} d_1 + d_2\,|v_1| & 0 & 0 \\ 0 & d_3 + d_4\,|v_2| & 0 \\ 0 & 0 & d_5 + d_6\,|v_3| \end{bmatrix} \begin{bmatrix} v_1 \\ v_2 \\ v_3 \end{bmatrix}, \\ N_2(w) &= \begin{bmatrix} g_1 + g_2\,|\omega_1| & 0 & 0 \\ 0 & g_3 + g_4\,|\omega_2| & 0 \\ 0 & 0 & g_5 + g_6\,|\omega_3| \end{bmatrix} \begin{bmatrix} \omega_1 \\ \omega_2 \\ \omega_3 \end{bmatrix}. \end{aligned} \tag{192}$$

E.3 Linear Parameterization

The assumed model for the aerodynamic damping terms in (192) were used to create the parameterization $Y_1(\hat{v})\theta_1$, $Y_2(\hat{\omega})\theta_2$ by utilizing A2 and invoking the estimated velocities $\hat{v}(t)$, $\hat{w}(t)$ given by

$$\begin{aligned} Y_1(\hat{v}) &= \begin{bmatrix} \hat{v}_1 & \hat{v}_1 \cdot |\hat{v}_1| & 0 & 0 & 0 & 0 \\ 0 & 0 & \hat{v}_2 & \hat{v}_2 \cdot |\hat{v}_2| & 0 & 0 \\ 0 & 0 & 0 & 0 & \hat{v}_3 & \hat{v}_3 \cdot |\hat{v}_3| \end{bmatrix}, \\ \theta_1 &= [d_1, d_2, d_3, d_4, d_5, d_6]^T = [0.065, 0.065, 0.065, 0.065, 0.065, 0.065]^T, \text{ and} \\ Y_2(\hat{\omega}) &= \begin{bmatrix} \hat{\omega}_1 & \hat{\omega}_1 \cdot |\hat{\omega}_1| & 0 & 0 & 0 & 0 \\ 0 & 0 & \hat{\omega}_2 & \hat{\omega}_2 \cdot |\hat{\omega}_2| & 0 & 0 \\ 0 & 0 & 0 & 0 & \hat{\omega}_3 & \hat{\omega}_3 \cdot |\hat{\omega}_3| \end{bmatrix}, \\ \theta_2 &= [g_1, g_2, g_3, g_4, g_5, g_6]^T = [0.065, 0.065, 0.065, 0.065, 0.065, 0.065]^T \end{aligned} \tag{193}$$

where the numerical values for the damping parameters are borrowed from [15]. To show the linear parmaterization of the equation (78) we first need to complete the derivative of $\bar{u}_1(t)$ in (79). The derivative $Y_1(\hat{v})\theta_1$ in (80) to match the derivative of the control input $u_1(t)$, $\dot{\bar{u}}_1\ (t)$, which is used for torque input $u_2(t)$ in (81) can be found as shown below

$$\begin{aligned} \frac{d}{dt}\left(Y_1(\hat{v})\theta_1\right) &= \begin{bmatrix} \dot{\hat{v}}_1 & \left(|\hat{v}_1| + \hat{v}_1 sgn(\hat{v}_1)\right)\dot{\hat{v}}_1 & 0 & 0 & 0 & 0 \\ 0 & 0 & \dot{\hat{v}}_2 & \left(|\hat{v}_2| + \hat{v}_2 sgn(\hat{v}_2)\right)\dot{\hat{v}}_2 & 0 & 0 \\ 0 & 0 & 0 & 0 & \dot{\hat{v}}_3 & \left(|\hat{v}_3| + \hat{v}_3 sgn(\hat{v}_3)\right)\dot{\hat{v}}_3 \end{bmatrix} \theta_1 \\ &= \begin{bmatrix} \dot{\hat{v}}_1 & 2\,|\hat{v}_1|\,\dot{\hat{v}}_1 & 0 & 0 & 0 & 0 \\ 0 & 0 & \dot{\hat{v}}_2 & 2\,|\hat{v}_2|\,\dot{\hat{v}}_2 & 0 & 0 \\ 0 & 0 & 0 & 0 & \dot{\hat{v}}_3 & 2\,|\hat{v}_3|\,\dot{\hat{v}}_3 \end{bmatrix} \theta_1 \\ &= \begin{bmatrix} \left(d_1 + 2d_2 \cdot |\hat{v}_1|\right)\dot{\hat{v}}_1 \\ \left(d_3 + 2d_4 \cdot |\hat{v}_2|\right)\dot{\hat{v}}_2 \\ \left(d_5 + 2d_6 \cdot |\hat{v}_3|\right)\dot{\hat{v}}_3 \end{bmatrix} \\ &= \begin{bmatrix} d_1 + 2d_2 \cdot |\hat{v}_1| & 0 & 0 \\ 0 & d_3 + 2d_4 \cdot |\hat{v}_2| & 0 \\ 0 & 0 & d_5 + 2d_6 \cdot |\hat{v}_3| \end{bmatrix} \begin{bmatrix} \dot{\hat{v}}_1 \\ \dot{\hat{v}}_2 \\ \dot{\hat{v}}_3 \end{bmatrix} \\ &= H_1\,\dot{\hat{v}} \end{aligned} \tag{194}$$

$$
\begin{aligned}
&= H_1\left(-S(\hat{\omega})\hat{v} + \frac{1}{m}(B_1u_1 + G - Y_1(\hat{v})\theta_1)\right) \\
&= H_1\left(-S(\hat{\omega})\hat{v} + \frac{1}{m}(B_1u_1 + G)\right) - H_1\frac{1}{m}Y_1(\hat{v})\theta_1
\end{aligned}
$$

where $H_1(\cdot) \in \Re^{3x3}$ is defined as

$$
H_1 = \begin{bmatrix} d_1 + 2d_2 \cdot |\hat{v}_1| & 0 & 0 \\ 0 & d_3 + 2d_4 \cdot |\hat{v}_2| & 0 \\ 0 & 0 & d_5 + 2d_6 \cdot |\hat{v}_3| \end{bmatrix}, \tag{195}
$$

and $\frac{d}{dt}|\hat{v}| = \dot{\hat{v}}\ sgn(\hat{v})$ and the first equation of the modeling equation were utilized. Substituting $\bar{u}_1(t)$ in (66) into $\dot{\hat{r}}\ (t)$ in (63) yields

$$
\dot{\hat{r}} = -k_r\hat{r} + \begin{bmatrix} -S(\hat{\omega})\hat{r}_p - \frac{1}{m}e_p \\ 0 \end{bmatrix} + B_\mu \begin{bmatrix} \hat{z} \\ 0 \end{bmatrix}. \tag{196}
$$

Then we substitute for $U(t)$ from (66) and for $\frac{d}{dt}U(t)$ from (80) and also substitute general error definitions from (56), (57), (196), and the derivative of $Y_1(\hat{v})\theta_1$ from (194) to yield

$$
\begin{aligned}
\dot{\bar{u}}_1 &= \frac{d}{dt}(B_\mu^{-1})\left(-k_r\hat{r} + \begin{bmatrix} -\frac{\alpha}{m}\hat{e}_v - \alpha(\frac{1}{m} - 1)R^T\dot{p}_d - G(R) - Y_1(\hat{v})\theta_1 + R^T\ddot{p}_d - \frac{1}{m}e_p \\ \omega_{zd} \end{bmatrix}\right) \\
&\quad -(B_\mu^{-1})k_r\left(-k_r\hat{r} + \begin{bmatrix} -S(\hat{\omega})\hat{r}_p - \frac{1}{m}e_p \\ 0 \end{bmatrix} + B_\mu \begin{bmatrix} \hat{z} \\ 0 \end{bmatrix}\right) \\
&\quad -(B_\mu^{-1})\begin{bmatrix} \frac{\alpha}{m}\left(-S(\hat{\omega})\hat{e}_v + G(R) + Y_1(\hat{v})\theta_1 - R^T\ddot{p}_d + B_1u_1\right) \\ 0 \end{bmatrix} \\
&\quad -(B_\mu^{-1})\begin{bmatrix} H_1\left(-S(\hat{\omega})\hat{v} + \frac{1}{m}(B_1u_1 + G(R))\right) - H_1\frac{1}{m}\hat{Y}_1(\hat{v})\theta_1 \\ 0 \end{bmatrix} \\
&\quad -(B_\mu^{-1})\begin{bmatrix} \frac{1}{m}\left(-S(\hat{\omega})e_p + \frac{1}{m}\hat{e}_v + (\frac{1}{m} - 1)R^T\dot{p}_d\right) \\ 0 \end{bmatrix} \\
&\quad -(B_\mu^{-1})\begin{bmatrix} S(\hat{\omega})\left(\frac{\alpha}{m}R^T\dot{p}_d - \alpha R^T\dot{p}_d - R^T\ddot{p}_d + mgR^TE_z\right) + \alpha\left(1 - \frac{1}{m}\right)R^T\ddot{p}_d + R^T\dddot{p}_d \\ \dot{\omega}_{zd} \end{bmatrix}.
\end{aligned} \tag{197}
$$

The $\hat{Y}_1(\hat{v})\theta_1$ terms in (197) are now grouped to yield

$$
\begin{aligned}
\dot{\bar{u}}_1 &= \frac{d}{dt}(B_\mu^{-1})\left(-k_r\hat{r} + \begin{bmatrix} -\frac{\alpha}{m}\hat{e}_v - \alpha(\frac{1}{m} - 1)R^T\dot{p}_d - G(R) + R^T\ddot{p}_d - \frac{1}{m}e_p \\ \omega_{zd} \end{bmatrix}\right) \\
&\quad -(B_\mu^{-1})k_r\left(-k_r\hat{r} + \begin{bmatrix} -S(\hat{\omega})\hat{r}_p - \frac{1}{m}e_p \\ 0 \end{bmatrix} + B_\mu \begin{bmatrix} \hat{z} \\ 0 \end{bmatrix}\right) \\
&\quad -(B_\mu^{-1})\begin{bmatrix} \frac{\alpha}{m}\left(-S(\hat{\omega})\hat{e}_v + G(R) - R^T\ddot{p}_d + B_1u_1\right) \\ 0 \end{bmatrix} \\
&\quad -(B_\mu^{-1})\begin{bmatrix} H_1\left(-S(\hat{\omega})\hat{v} + \frac{1}{m}(B_1u_1 + G(R))\right) \\ 0 \end{bmatrix} \\
&\quad -(B_\mu^{-1})\begin{bmatrix} \frac{1}{m}\left(-S(\hat{\omega})e_p + \frac{1}{m}\hat{e}_v + (\frac{1}{m} - 1)R^T\dot{p}_d\right) \\ 0 \end{bmatrix}
\end{aligned} \tag{198}
$$

$$-(B_\mu^{-1})\begin{bmatrix} S(\hat{\omega})\left(\frac{\alpha}{m}R^T\dot{p}_d - \alpha R^T\dot{p}_d - R^T\,\ddot{p}_d + mgR^TE_z\right) + \alpha\left(1-\frac{1}{m}\right)R^T\,\ddot{p}_d + R^T\,\dddot{p}_d \\ \dot{\omega}_{zd} \end{bmatrix}$$
$$-\frac{d}{dt}(B_\mu^{-1})\begin{bmatrix} Y_1(\hat{v})\theta_1 \\ 0 \end{bmatrix} + (B_\mu^{-1})\begin{bmatrix} \frac{1}{m}H_1\hat{Y}_1(\hat{v})\theta_1 \\ 0 \end{bmatrix} - (B_\mu^{-1})\begin{bmatrix} \frac{\alpha}{m}Y_1(\hat{v})\theta_1 \\ 0 \end{bmatrix}.$$

Hence, the equation (198) can be made more manageable in the form

$$\dot{\bar{u}}_1 = \frac{d}{dt}(B_\mu^{-1})\phi_a(p,R,\hat{v},\hat{\omega}) + (B_\mu^{-1})\phi_b(p,R,\hat{v},\hat{\omega}) + \left(\frac{d}{dt}(B_\mu^{-1})\phi_c + (B_\mu^{-1})\phi_d(\hat{v})\right)\hat{Y}_1(\hat{v})\theta_1 \tag{199}$$

where by the variables $\phi_a(p,R,\hat{v},\hat{\omega})$, $\phi_b(p,R,\hat{v},\hat{\omega}) \in \Re^4$ have the definitions

$$\phi_a(p,R,\hat{v},\hat{\omega}) = -k_r\hat{r} + U1, \tag{200}$$
$$\phi_b(p,R,\hat{v},\hat{\omega}) = -k_rU2 - U3 - U4 - U5 - U6 \tag{201}$$
$$\text{where } U1 = \begin{bmatrix} -\frac{\alpha}{m}\hat{e}_v - \alpha(\frac{1}{m}-1)R^T\dot{p}_d - G(R) + R^T\,\ddot{p}_d - \frac{1}{m}e_p \\ \omega_{zd} \end{bmatrix},$$
$$U2 = \left(-k_r\hat{r} + \begin{bmatrix} -S(\hat{\omega})\hat{r}_p - \frac{1}{m}e_p \\ 0 \end{bmatrix} + B_\mu\begin{bmatrix} \hat{z} \\ 0 \end{bmatrix}\right),$$
$$U3 = \begin{bmatrix} \frac{\alpha}{m}\left(-S(\hat{\omega})\hat{e}_v + B_1u_1 + G(R) - R^T\,\ddot{p}_d\right) \\ 0 \end{bmatrix}, \tag{202}$$
$$U4 = \begin{bmatrix} H_1\left(-S(\hat{\omega})\hat{v} + \frac{1}{m}(B_1u_1 + G(R))\right) \\ 0 \end{bmatrix},$$
$$U5 = \begin{bmatrix} \frac{1}{m}\left(-S(\hat{\omega})e_p + \frac{1}{m}\hat{e}_v + (\frac{1}{m}-1)R^T\dot{p}_d\right) \\ 0 \end{bmatrix},$$
$$U6 = \begin{bmatrix} S(\hat{\omega})\left(\frac{\alpha}{m}R^T\dot{p}_d - \alpha R^T\dot{p}_d - R^T\,\ddot{p}_d + mgR^TE_z\right) + \alpha\left(1-\frac{1}{m}\right)R^T\,\ddot{p}_d + R^T\,\dddot{p}_d \\ \dot{\omega}_{zd} \end{bmatrix},$$

in which $k_r \in \Re^{4x4}$ is

$$k_r = \begin{bmatrix} k_{r1} & 0 & 0 & 0 \\ 0 & k_{r1} & 0 & 0 \\ 0 & 0 & k_{r1} & 0 \\ 0 & 0 & 0 & k_{r2} \end{bmatrix}, \tag{203}$$

and $\phi_c(\cdot) \in \Re^{4x3}$ and $\phi_d(\hat{v}) \in \Re^{4x3}$ are two regression matrices given by

$$\phi_c = \begin{bmatrix} -I_3 \\ O_{1x3} \end{bmatrix}, \tag{204}$$
$$\phi_d = \left(-\frac{\alpha}{m}I_4\right)\begin{bmatrix} I_3 \\ O_{1x3} \end{bmatrix} + \begin{bmatrix} \frac{1}{m}H_1 \\ O_{1x3} \end{bmatrix}. \tag{205}$$

Note that the following manipulation was used to facilitate the form of $\phi_c \in \Re^{4x3}$ and $\phi_d(\hat{v}) \in \Re^{4x3}$:

$$\begin{bmatrix} Y_1(\hat{v})\theta_1 \\ 0 \end{bmatrix} = \begin{bmatrix} I_3 \\ O_{1x3} \end{bmatrix} Y_1(\hat{v})\theta_1 = B_z^TY_1(\hat{v})\theta_1 \in \Re^4.$$

Therefore, the definition of $Y_3(p,R,\hat{v},\hat{\omega})\theta_3$ in (76) can now be implemented using (199) and (193) to produce the parameterization $Y_3(p,R,\hat{v},\hat{\omega}) \in \Re^{3x27}$ and $\theta_3 \in \Re^{27}$. The final form is given by

$Y_3(p, R, \hat{v}, \hat{\omega}) = [Y_{31}, Y_{32}, Y_{33}, Y_{34}, Y_{35}, Y_{36}]$, with elements

$$
\begin{aligned}
Y_{31} &= \begin{bmatrix} \frac{\phi_{b2}}{\delta_3} & \omega_2\omega_3 & -\omega_2\omega_3 \\ -\omega_1\omega_3 & -\frac{\phi_{b1}}{\delta_3} & \omega_1\omega_3 \\ \omega_1\omega_2 & -\omega_1\omega_2 & \left(\frac{\phi_{a1}}{\delta_3}\left(\frac{\dot{s\phi}}{c\phi}\right) - \left(\frac{\dot{c\theta}}{c\phi}\right)\phi_{a4} + \frac{\phi_{b1}}{\delta_3}t\phi - \frac{c\theta}{c\phi}\phi_{b4}\right) \end{bmatrix}, \\
Y_{32} &= \begin{bmatrix} \omega_1 & \omega_1|\omega_1| & 0 & 0 & 0 & 0 \\ 0 & 0 & \omega_2 & \omega_2|\omega_2| & 0 & 0 \\ 0 & 0 & 0 & 0 & \omega_3 & \omega_3|\omega_3| \end{bmatrix}, \\
Y_{33} &= \begin{bmatrix} \frac{\phi_{d21}}{\delta_3}v_1 & 0 & 0 \\ 0 & -\frac{\phi_{d11}}{\delta_3}v_1 & 0 \\ 0 & 0 & \left(-\frac{1}{\delta_3}\left(\frac{\dot{s\phi}}{c\phi}\right) + \frac{\phi_{d11}t\phi}{\delta_3} - \frac{\phi_{d41}c\theta}{c\phi}\right)v_1 \end{bmatrix}, \\
Y_{34} &= \begin{bmatrix} \frac{\phi_{d21}}{\delta_3}v_1|v_1| & 0 & 0 \\ 0 & -\frac{\phi_{d11}}{\delta_3}v_1|v_1| & 0 \\ 0 & 0 & \left(-\frac{1}{\delta_3}\left(\frac{\dot{s\phi}}{c\phi}\right) + \frac{\phi_{d11}t\phi}{\delta_3} - \frac{\phi_{d41}c\theta}{c\phi}\right)v_1|v_1| \end{bmatrix}, \\
Y_{35} &= \begin{bmatrix} \frac{\phi_{d22}}{\delta_3}v_2 & 0 & 0 & \frac{\phi_{d22}}{\delta_3}v_2|v_2| & 0 & 0 \\ 0 & -\frac{\phi_{d12}}{\delta_3}v_2 & 0 & 0 & -\frac{\phi_{d12}}{\delta_3}v_2|v_2| & 0 \\ 0 & 0 & \left(\frac{\phi_{d12}t\phi}{\delta_3} - \frac{\phi_{d42}c\theta}{c\phi}\right)v_2 & 0 & 0 & \left(\frac{\phi_{d12}t\phi}{\delta_3} - \frac{\phi_{d42}c\theta}{c\phi}\right)v_2|v_2| \end{bmatrix}, \\
Y_{36} &= \begin{bmatrix} \frac{\phi_{d23}}{\delta_3}v_3 & 0 & 0 & \frac{\phi_{d23}}{\delta_3}v_3|v_3| & 0 & 0 \\ 0 & -\frac{\phi_{d13}}{\delta_3}v_3 & 0 & 0 & -\frac{\phi_{d13}}{\delta_3}v_3|v_3| & 0 \\ 0 & 0 & \left(\frac{\phi_{d13}t\phi}{\delta_3} - \frac{\phi_{d43}c\theta}{c\phi}\right)v_3 & 0 & 0 & \left(\frac{\phi_{d13}t\phi}{\delta_3} - \frac{\phi_{d43}c\theta}{c\phi}\right)v_3|v_3| \end{bmatrix},
\end{aligned}
\tag{206}
$$

and by $\theta_3 = [\theta_{31}, \theta_{32}, \theta_{33}, \theta_{34}]^T$ with elements given by

$$
\begin{aligned}
\theta_{31} &= \begin{bmatrix} J_{11} & J_{22} & J_{33} & g_1 & g_2 & g_3 & g_4 & g_5 & g_6 \end{bmatrix}, \\
\theta_{32} &= \begin{bmatrix} J_{11}d_1 & J_{22}d_1 & J_{33}d_1 & J_{11}d_2 & J_{22}d_2 & J_{33}d_2 \end{bmatrix}, \\
\theta_{33} &= \begin{bmatrix} J_{11}d_3 & J_{22}d_3 & J_{33}d_3 & J_{11}d_4 & J_{22}d_4 & J_{33}d_4 \end{bmatrix}, \\
\theta_{34} &= \begin{bmatrix} J_{11}d_5 & J_{22}d_5 & J_{33}d_5 & J_{11}d_6 & J_{22}d_6 & J_{33}d_6 \end{bmatrix}.
\end{aligned}
\tag{207}
$$

F Development of Centrifugal/Coriolis terms

Consider the Centrifugal/Coriolis force equations in (52), it can be rewritten as follows

$$N^*(R, T, \dot{x})\dot{x}_o - N^*(R, T, \dot{x}_o)\dot{x}_o = [N^*(R, T, \dot{x}) - N^*(R, T, \dot{x}_o)]\,\dot{x}_o.$$

First we consider the first term, $N^*(R, T, \dot{x})$, on the right-hand side of above equation

$$N^*(R, T, \dot{x}) \triangleq D^T(R, T)\left(\bar{C}(R, T)D(R, T) - \bar{M}\bar{D}(R, T, \dot{x})\right) \tag{208}$$

where

$$\bar{C}(R, T)D(R, T) - \bar{M}\bar{D}(R, T, \dot{x})$$

$$
\begin{aligned}
&= \begin{bmatrix} -mS(\omega) & O_{3x3} \\ O_{3x3} & S(J\omega) \end{bmatrix} \begin{bmatrix} R^T & O_{3x3} \\ O_{3x3} & T^{-1}(\Theta) \end{bmatrix} - \begin{bmatrix} mI_3 & O_{3x3} \\ O_{3x3} & J \end{bmatrix} \begin{bmatrix} \frac{d}{dt}(R^T) & O_{3x3} \\ O_{3x3} & \frac{d}{dt}(T^{-1}(\Theta)) \end{bmatrix} \\
&= \begin{bmatrix} -mS(\omega)R^T & O_{3x3} \\ O_{3x3} & S(J\omega)T^{-1}(\Theta) \end{bmatrix} - \begin{bmatrix} m\frac{d}{dt}(R^T) & O_{3x3} \\ O_{3x3} & J\frac{d}{dt}(T^{-1}(\Theta)) \end{bmatrix} \\
&= \begin{bmatrix} -mS(\omega)R^T - m\frac{d}{dt}(R^T) & O_{3x3} \\ O_{3x3} & S(J\omega)T^{-1}(\Theta) - J\frac{d}{dt}(T^{-1}(\Theta)) \end{bmatrix} \\
&= \begin{bmatrix} O_{3x3} & O_{3x3} \\ O_{3x3} & S(J\omega)T^{-1}(\Theta) - J\frac{d}{dt}(T^{-1}(\Theta)) \end{bmatrix}.
\end{aligned}
$$

Then, (208) becomes

$$
\begin{aligned}
N^*(R,T,\dot{x}) &\triangleq \begin{bmatrix} R & O_{3x3} \\ O_{3x3} & T^{-T}(\Theta) \end{bmatrix} \left(\begin{bmatrix} O_{3x3} & O_{3x3} \\ O_{3x3} & S(J\omega)T^{-1}(\Theta) - J\frac{d}{dt}(T^{-1}(\Theta)) \end{bmatrix} \right) \\
&= \begin{bmatrix} O_{3x3} & O_{3x3} \\ O_{3x3} & T^{-T}(\Theta)\left[S(J\omega)T^{-1}(\Theta) - J\frac{d}{dt}(T^{-1}(\Theta))|_{\dot{\Theta}}\right] \end{bmatrix}. \qquad (209)
\end{aligned}
$$

In a same fashion, we can obtain

$$
N^*(R,T,\dot{x}_o) = \begin{bmatrix} O_{3x3} & O_{3x3} \\ O_{3x3} & T^{-T}(\Theta)\left[S(J\omega_o)T^{-1}(\Theta) - J\frac{d}{dt}(T^{-1}(\Theta))|_{\dot{\Theta}=\dot{\Theta}_o}\right] \end{bmatrix}. \qquad (210)
$$

Then, the difference between (209) and (208) yields

$$
\begin{aligned}
&N^*(R,T,\dot{x}) - N^*(R,T,\dot{x}_o) \\
&= \begin{bmatrix} O_{3x3} & O_{3x3} \\ O_{3x3} & T^{-T}(\Theta)\left[S(J\omega)T^{-1}(\Theta) - J\frac{d}{dt}(T^{-1}(\Theta))\right] - T^{-T}(\Theta)\left[S(J\omega_o)T^{-1}(\Theta) - J\frac{d}{dt}(T^{-1}(\Theta))|_{\dot{\Theta}=\dot{\Theta}_o}\right] \end{bmatrix} \\
&= \begin{bmatrix} O_{3x3} & O_{3x3} \\ O_{3x3} & T^{-T}(\Theta)\left[S(J\omega)T^{-1}(\Theta) - S(J\omega_o)T^{-1}(\Theta)\right] + T^{-T}(\Theta)\left[-J\frac{d}{dt}(T^{-1}(\Theta)) + J\frac{d}{dt}(T^{-1}(\Theta))|_{\dot{\Theta}=\dot{\Theta}_o}\right] \end{bmatrix}. \qquad (211)
\end{aligned}
$$

The first term in the last matrix in (211) yields

$$
\begin{aligned}
& T^{-T}(\Theta)\left[S(J\omega)T^{-1}(\Theta) - S(J\omega_o)T^{-1}(\Theta)\right] \\
=\ & T^{-T}(\Theta)S(J\omega - J\omega_o)T^{-1}(\Theta) \\
=\ & T^{-T}(\Theta)S(JT^{-1}(\Theta)(\dot{\Theta} - \dot{\Theta}_o))T^{-1}(\Theta) \\
=\ & T^{-T}(\Theta)S(JT^{-1}(\Theta)s\_\Theta)T^{-1}(\Theta) \qquad (212)
\end{aligned}
$$

where from the definition in (41) we can represent

$$
s = \dot{x} - \dot{x}_o = \begin{bmatrix} \dot{p} - \dot{p}_o \\ \dot{\Theta} - \dot{\Theta}_o \end{bmatrix} \triangleq \begin{bmatrix} s\_p \\ s\_\Theta \end{bmatrix},
$$

by defining as

$$
s\_p = \dot{p} - \dot{p}_o \in \Re^3 \text{ and } s\_\Theta = \dot{\Theta} - \dot{\Theta}_o \in \Re^3.
$$

The second term in the last matrix in (211) yields using the (138)

$$
T^{-T}(\Theta)\left[-J\frac{d}{dt}(T^{-1}(\Theta)) + J\frac{d}{dt}(T^{-1}(\Theta))|_{\dot{\Theta}=\dot{\Theta}_o}\right]
$$

$$
\begin{aligned}
&= T^{-T}(\Theta)\left(-J\frac{\partial}{\partial\Theta}(T^{-1}(\Theta))\dot{\Theta} + J\frac{\partial}{\partial\Theta}(T^{-1}(\Theta))\dot{\Theta}_o\right)\\
&= -T^{-T}(\Theta)J\frac{\partial}{\partial\Theta}(T^{-1}(\Theta))\left(\dot{\Theta}-\dot{\Theta}_o\right)\\
&= -T^{-T}(\Theta)J\frac{\partial}{\partial\Theta}(T^{-1}(\Theta))s\_\Theta \qquad (213)
\end{aligned}
$$

where

$$
\begin{aligned}
\frac{d}{dt}(T^{-1}(\Theta)) &= \frac{\partial}{\partial\Theta}(T^{-1}(\Theta))\dot{\Theta} \in \Re^{3x3} \qquad (214)\\
\frac{\partial}{\partial\Theta}(T^{-1}(\Theta)) &\in \Re^{3x3x3} \text{ as a tensor.} \qquad (215)
\end{aligned}
$$

Thus, the matrix (211) yields

$$
\begin{aligned}
&N^*(R,T,\dot{x}) - N^*(R,T,\dot{x}_o)\\
&= \begin{bmatrix} O_{3x3} & O_{3x3} \\ O_{3x3} & T^{-T}(\Theta)S(JT^{-1}(\Theta)s\_\Theta)T^{-1}(\Theta) - T^{-T}(\Theta)J\frac{\partial}{\partial\Theta}(T^{-1}(\Theta))s\_\Theta \end{bmatrix}. \qquad (216)
\end{aligned}
$$

Hence, the Centrifugal/Coriolis equations in (52) can be defined as

$$
\begin{aligned}
&N^*(R,T,\dot{x})\dot{x}_o - N^*(R,T,\dot{x}_o)\dot{x}_o\\
&= \left(N^*(R,T,\dot{x}) - N^*(R,T,\dot{x}_o)\right)\dot{x}_o\\
&= \begin{bmatrix} O_{3x3} & O_{3x3} \\ O_{3x3} & T^{-T}(\Theta)S(JT^{-1}(\Theta)s\_\Theta)T^{-1}(\Theta) - T^{-T}(\Theta)J\frac{\partial}{\partial\Theta}(T^{-1}(\Theta))s\_\Theta \end{bmatrix}\dot{x}_o\\
&= \begin{bmatrix} O_{3x3} & O_{3x3} \\ O_{3x3} & T^{-T}(\Theta)S(JT^{-1}(\Theta)s\_\Theta)T^{-1}(\Theta) - T^{-T}(\Theta)\bar{T}(J,\Theta,s\_\Theta) \end{bmatrix}\begin{bmatrix} \dot{p}_o \\ \dot{\Theta}_o \end{bmatrix}\\
&= \begin{bmatrix} O_{3x1} \\ T^{-T}(\Theta)S(JT^{-1}(\Theta)s\_\Theta)T^{-1}(\Theta)\dot{\Theta}_o - T^{-T}(\Theta)\bar{T}(J,\Theta,s\_\Theta)\dot{\Theta}_o \end{bmatrix}\\
&= \begin{bmatrix} O_{3x1} \\ -T^{-T}(\Theta)S(T^{-1}(\Theta)\dot{\Theta}_o)JT^{-1}(\Theta)s\_\Theta - T^{-T}(\Theta)T_c(J,\Theta,\dot{\Theta}_o)s\_\Theta \end{bmatrix}\\
&= \begin{bmatrix} O_{3x3} & O_{3x3} \\ O_{3x3} & T^{-T}(\Theta)\left(-S(T^{-1}(\Theta)\dot{\Theta}_o)JT^{-1}(\Theta) - T_c(J,\Theta,\dot{\Theta}_o)\right) \end{bmatrix}\begin{bmatrix} s\_p \\ s\_\Theta \end{bmatrix}\\
&= N_c^*(R,T,\dot{x}_o)s \qquad (217)
\end{aligned}
$$

where

$$
N_c^*(R,T,\dot{x}_o) = \begin{bmatrix} O_{3x3} & O_{3x3} \\ O_{3x3} & T^{-T}(\Theta)\left(-S(T^{-1}(\Theta)\dot{\Theta}_o)JT^{-1}(\Theta) - T_c(J,\Theta,\dot{\Theta}_o)\right) \end{bmatrix}, \qquad (218)
$$

and the followings are utilized

$$
\begin{aligned}
\bar{T}(J,\Theta,s\_\Theta) &= J\frac{\partial}{\partial\Theta}(T^{-1}(\Theta))s\_\Theta,\\
T_c(J,\Theta,\dot{\Theta}_o)s\_\Theta &= \bar{T}(J,\Theta,s\_\Theta)\dot{\Theta}_o.
\end{aligned}
$$

G Figures

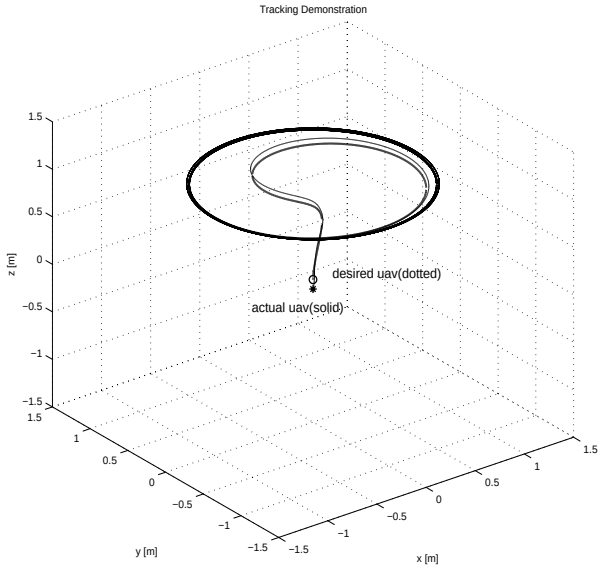

Figure 3: Output Feedback Tracking Demonstration

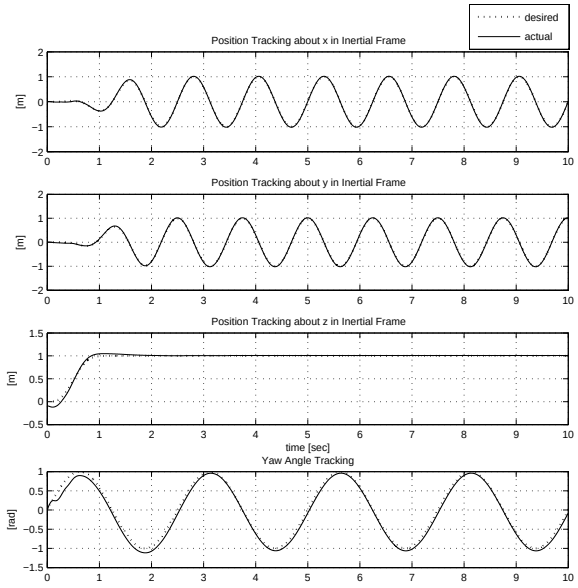

Figure 4: Position and Yaw Tracking at Each Axis

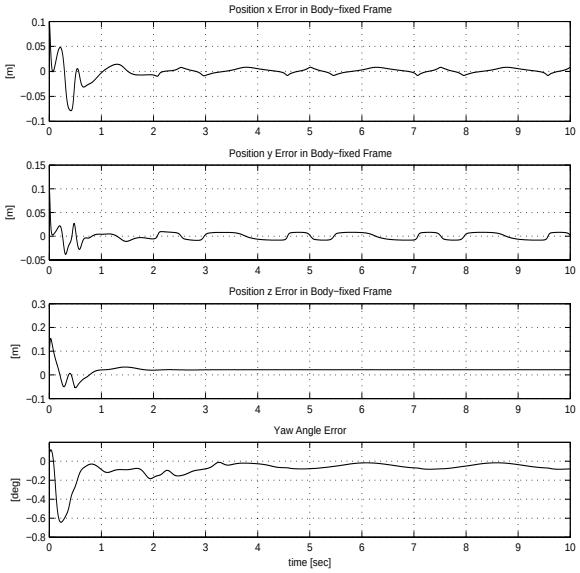

Figure 5: Position and Yaw Tracking Errors

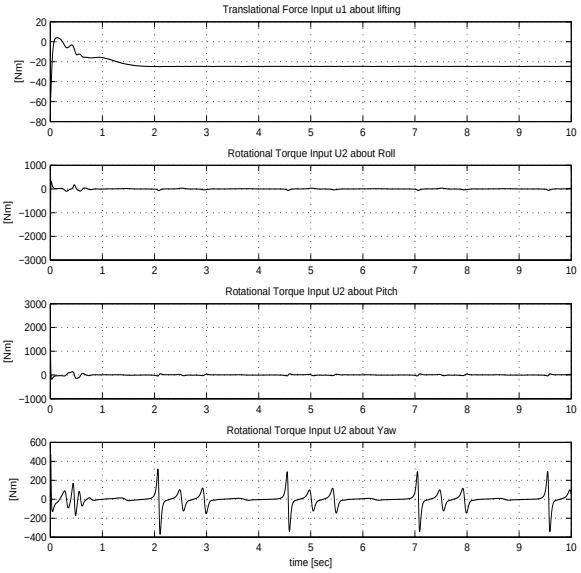

Figure 6: Control Inputs : Force and Torques

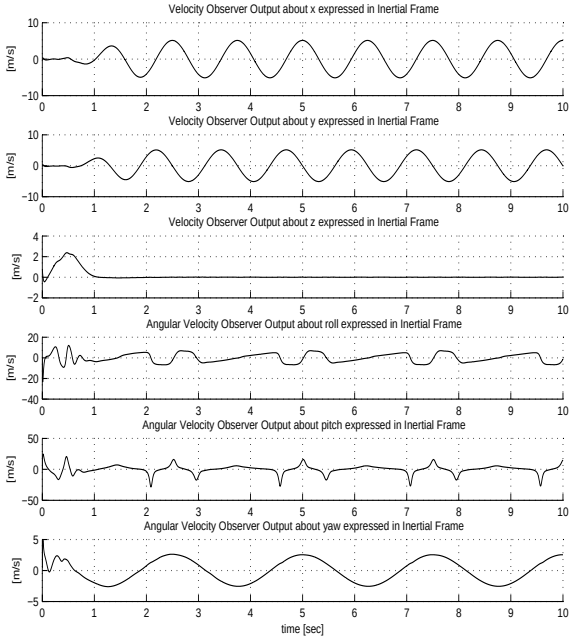

Figure 7: Velocity Observer Output